

INFLUENCE OF VEGETATION ON NIAGARA ESCARPMENT EROSION

ASSESSING THE IMPACT OF VEGETATION ON EROSION PROCESSES ON THE
NIAGARA ESCARPMENT IN THE HAMILTON REGION, CANADA

By Allie Ellis, B.A.

A Thesis Submitted to the School of
Graduate Studies in Partial Fulfilment
of the Requirements for the Degree
Master of Science

McMaster University © Copyright by
Allie Ellis, April 2022

M.Sc. Thesis – A. Ellis; McMaster University – Environmental Science.

McMaster University MASTER OF SCIENCE (2022) Hamilton, Ontario (Environmental Science)

TITLE: Assessing the impact of vegetation on erosion processes on the Niagara Escarpment in the Hamilton region, Canada AUTHOR: Allie Ellis, B.A. (McMaster University)
SUPERVISOR: Professor C. Eyles NUMBER OF PAGES: xi, 72

Lay Abstract

This research examines the impact of vegetation growth on erosion processes on the Niagara Escarpment in Hamilton, Ontario. The slope of the escarpment face exerts an important control on vegetation growth which in turn affects slope stability. Documentation of the dominant vegetation species at two research sites allows the identification of three distinct vegetation zones on the upper plateau, bedrock face, and sloping talus. The movement of tree trunks in response to air movement was also measured for several days in the months of March, May, October and November. Results show that the movement of two monitored deciduous trees was most strongly correlated to wind direction, while the movement of a coniferous tree was strongly correlated to changes in wind speed. All monitored trees were strongly influenced by daily cycles of air movement which were greatest around noon. This research identifies factors that influence both vegetation growth and slope stability on the Niagara Escarpment and may be used to develop effective erosion protection and mitigation strategies.

Abstract

The stability of the Niagara Escarpment is of critical importance to residents of Hamilton, Ontario as it bisects and divides the lower downtown core from upper residential and commercial areas. The frequency of large rockfalls and debris slides from the exposed escarpment face has resulted in reoccurring road closures that connect these two areas and has prompted the city to seek information on the processes affecting escarpment erosion and slope stability. The research reported here examines the relationship between tree and plant growth on bedrock stability by investigating relationships between species abundance and slope profile, and the potential movement of tree roots growing in rock fractures.

The contributing factors of tree growth to physical weathering processes on highly fractured bedrock remain largely unknown; however, plants are suggested to play a key role in weathering processes in the critical zone. Bedrock structure and lithology influence the establishment of vegetation, and vegetation in turn exploits bedrock joints, fractures, and bedding planes, exacerbating physical and biomechanical weathering processes. In this study, vegetation characteristics observed on different parts of the escarpment face were documented and categorized into three distinct biophysical zones: upper and intermediary plateau, bedrock face, and sloping talus. Tree growth, with the potential to enhance bedrock disaggregation through the transfer of tree bole movement to roots exploiting bedrock fractures, was particularly prevalent on areas of sloping talus. To document the potential for bedrock disaggregation through tree bole movement, triaxial accelerometers were mounted on the boles of three different tree species growing along the escarpment in Hamilton. Sampled trees varied in geographic location to allow identification of the relationship between tree bole movement, wind speed, and dominant wind direction. Both deciduous and coniferous species were monitored to determine the impacts of canopy architecture on tree sway in response to wind. Monitoring took place over several days in the months of March, May, September, and November. Recorded tree bole movement (tilt) varied between deciduous and coniferous tree species; wind speed was strongly correlated to tilt of the coniferous tree, and wind direction was strongly correlated to tilt of the deciduous trees. Overall tree bole movement was strongly influenced by diurnal cycles of air movement and was greatest in the hours around mid-day.

The outcomes of this research will form an integral component of an erosion-risk assessment study conducted, in part, for the City of Hamilton and will facilitate the design and development of vegetation management strategies for the Niagara Escarpment that may reduce erosion processes and potential damages to impacted citizens and businesses.

Acknowledgments

I would like to express my gratitude to Dr. Carolyn Eyles, my research supervisor, for their patient guidance, enthusiastic encouragement and useful critiques.

I would also like to thank James Wagner of Oregon Research Electronics (ORE) for their advice and assistance in my accelerometer data analysis.

Finally, I wish to thank my family and friends for their amazing support and encouragement throughout the entirety of my study, I could not have done this without you all.

Table of Contents

ABSTRACT.....	II
ACKNOWLEDGEMENTS.....	III
TABLE OF CONTENTS.....	VI
LIST OF FIGURES & TABLES.....	VII
1.0 INTRODUCTION	1
1.1 OBJECTIVES.....	5
1.2 GEOLOGICAL SETTING	6
1.3 GEOLOGY OF THE NIAGARA ESCARPMENT IN HAMILTON	6
1.4 VEGETATION CHARACTERISTICS OF THE NIAGARA ESCARPMENT IN HAMILTON	9
2.0 VEGETATION AND SLOPE EROSION	12
2.1 ROOT GROWTH IN FRACTURED BEDROCK	15
3.0 STUDY DESIGN.....	17
3.1 METHODS	17
3.1.1 Vegetation Survey	17
3.1.2 Tree Sway Measurement	19
3.1.3 Wind Data	21
3.1.4 Canopy Survey	22
3.2 ACCELEROMETER SENSOR CALIBRATION.....	22
3.2.1 Field Calibration.....	22
3.2.2 Accelerometer Offset Calibration	24
3.2.3 Net Total Tilt Displacement.....	26
3.3 DATA ANALYSIS	27
3.3.1 Statistical Analysis	29
4.0 RESULTS	30
4.1 VEGETATION CATALOGUE	30
4.1.1 Upper Plateau	32
4.1.2 Bedrock Face.....	32
4.1.3 Sloping Talus.....	33
4.2 WIND-INDUCED SWAY	34
4.2.1 Acceleration Trends	35
4.2.1.1 Diurnal movement.....	36
4.2.1.2 Data correction.....	41
4.2.1.3 Seasonal movement.....	42
4.3 ENVIRONMENTAL VARIABLES AND ACCELERATION	42
4.3.1 Wind Speed	42
4.3.2 Wind Direction.....	44
4.3.3 Canopy Cover.....	47
5.0 DISCUSSION	51
5.1 VEGETATION COMMUNITIES	51
5.2 SLOPE STABILIZATION	52
5.2.1 Tree Growth on Sloping Ground.....	53
5.2.2 Species Suitability	53
5.3 TREE BOLE TILT	56

5.3.1	Factors	56
5.4	CONCLUSIONS	59
5.4.1	Major Findings	59
5.4.2	Limitations	62
5.4.3	Future Research.....	63
BIBLIOGRAPHY		64
APPENDICES.....		70
APPENDIX A. ACCELEROMETER DISCREPENCIES		70
APPENDIX B. ACCELEROMETER LIMITATIONS		72

List of Figures

FIGURE 1: (A) GEOGRAPHIC EXTENT OF THE NIAGARA ESCARPMENT (GREEN) WITHIN EASTERN NORTH AMERICA. THE ESCARPMENT EXTENDS FROM WESTERN NEW YORK STATE, THROUGH ONTARIO, MICHIGAN, AND CENTRAL WISCONSIN. THE LOCATION OF HAMILTON, ONTARIO IS INDICATED BY A STAR (LEE, 2020). (B) MAP DEPICTING REGIONAL FIELDWORK LOCATIONS (BLACK CIRCLES) IN THE CITY OF HAMILTON AND THEIR POSITION ON THE NIAGARA ESCARPMENT (RED OUTLINE). GREEN DOTS HIGHLIGHT THE PLACEMENT OF ACCELEROMETER EQUIPMENT - TWO AT THE ROCKCLIFFE TRAIL LOCATION AND ONE AT THE CHEDOKE RADIAL TRAIL LOCATION; YELLOW STAR INDICATES THE LOCATION OF THE ROYAL BOTANICAL GARDENS (RBG) WEATHER STATION.	2
FIGURE 2: EARLY SILURIAN PALEO GEOGRAPHY RELATIVE TO PRESENT-DAY EROSIONAL BOUNDARIES INCLUDING THE APPALACHIAN FORELAND BASIN, MICHIGAN INTRACRATONIC BASIN AND THE ALGONQUIN-FINDLAY ARCHES (INDICATED BY THE THICK PINK LINES). THE DASHED YELLOW LINE REPRESENTS THE GEOGRAPHIC EXTENT OF THE NIAGARA ESCARPMENT IN RELATION TO THE BASINS, AND SUB-BASIN BOUNDARIES OF THE EARLY SILURIAN PALEO GEOGRAPHY (REPRODUCED FROM BRUNTON & BRINTNELL, 2020, WITH PERMISSION).	3
FIGURE 3: ACCESS ROADWAYS CUTTING THROUGH THE NIAGARA ESCARPMENT IN HAMILTON AND ASSOCIATED EROSION OF STEEP MARGINAL SLOPES (A) TOP OF THE JOLLEY CUT ROADWAY AND VIEW OF LOWER DOWNTOWN CORE, (B) SMALL BEDROCK SLIDE ALONG THE JOLLEY CUT, (C,D) FAILED INFRASTRUCTURE INSTALLED TO PREVENT EROSION ALONG THE SHERMAN CUT ROADWAY (LEE, 2018).	5
FIGURE 4: THE MAJOR STRATIGRAPHIC GROUPS, AND FORMATIONS EXPOSED ALONG THE NIAGARA ESCARPMENT IN HAMILTON, ONTARIO (LEE, PER. COM.)	8
FIGURE 5: THE PROVINCE OF ONTARIO, CANADA SHOWING THE THREE ECOZONES (UPPER: HUDSON BAY LOWLANDS, ONTARIO SHIELD, MIXEDWOOD PLAINS), AND THE THREE MAIN ECOREGIONS IN SOUTHERN ONTARIO (LOWER) INDICATED BY COLOUR AND LETTER/NUMBER CODES. THE YELLOW STAR INDICATES THE LOCATION OF HAMILTON, ONTARIO WITHIN THE LAKE ERIE-LAKE ONTARIO ECOREGION (ADAPTED FROM THE ECOLOGICAL LAND CLASSIFICATION PRIMER, (2007) BY ONTARIO.CA).	10
FIGURE 6: VERTICAL TRANSECT OF ESCARPMENT VEGETATION IN ALONG THE CHEDOKE RADIAL TRAIL, HAMILTON. PATTERNS OF PLANT GROWTH AND DEVELOPMENT CAN BE RELATED TO THE POSITION ON THE ESCARPMENT: UPPER PLATEAU, BEDROCK FACE, AND SLOPING TALUS.	11
FIGURE 7: VEGETATION GROWING ON BEDROCK ALONG THE NIAGARA ESCARPMENT IN HAMILTON: (A) LARGE ROOTS OF A MATURE TREE REMAIN INTACT AFTER FAILURE OF HIGHLY-FRACTURED UNDERLYING BEDROCK, (B) COLLAPSE OF FRACTURED BEDROCK BLOCKS BENEATH AN OVERLYING SOIL AND VEGETATION LAYER, (C) GROWTH POSITION OF AN ESTABLISHED TREE ON THE ESCARPMENT FACE. RED ARROWS HIGHLIGHT AREAS OF PREVIOUS BEDROCK EROSION, EVIDENT BY THE SPATIAL GAPS BETWEEN TREE ROOTS AND THE UNDERLYING SURFACE.	14
FIGURE 8: (MAP) THE GEOGRAPHIC LOCATIONS OF STUDY SITES ALONG THE NIAGARA ESCARPMENT IN HAMILTON (BLACK CIRCLES). GREEN DOTS INDICATE THE PLACEMENT OF ACCELEROMETER UNITS (B1, B2, R1). THE AL101 ACCELEROMETER UNITS INSTALLED ON THE TREES ARE INDICATED BY RED ARROWS; R1 (SUGAR MAPLE), B1 (RED OAK), AND B2 (WHITE CEDAR).	19
FIGURE 9: INTERNAL CIRCUIT BOARD OF THE AL101 ACCELEROMETER MANUFACTURED BY OREGON RESEARCH ELECTRONICS (ORE). THE BATTERY HOLDERS, MICRO-SD HOLDER, AND USB PORT ARE INDICATED BY RED ARROWS, AND COVER SCREW LOCATIONS ARE CIRCLED ALONG THE PERIMETER OF THE CONTAINER.	21

FIGURE 10: (A) WOODEN HOUSING CONTAINER MOUNTED TO A TREE BOLE WITH WHITE PLASTIC ZIP TIES AND SEALED WITH A SMALLER, BLACK ZIP TIE DURING A TRIAL OF RESEARCH EQUIPMENT, (B) INTERIOR VIEW OF WOODEN HOUSING CONTAINER AND THE POSITION OF THE AL101 DURING FIELD RESEARCH, (C) WOODEN HOUSING CONTAINER AND AL101 INSTALLED AT THE CHEDOKE RADIAL TRAIL FIELD SITE ON A SUGAR MAPLE (*ACER SACCHARUM*) ~2.7M FROM THE ROOT BASE. THE RED CIRCLE INDICATES THE LOCATION OF THE AL101 AND WOODEN HOUSING CONTAINER.....23

FIGURE 11: ACCELEROMETER R1 IN THE SIX CANONICAL POSITIONS USED TO CALCULATE OFFSET FOR EACH AXIS (X, Y, Z). THE ACCELEROMETER WAS ROTATED THROUGH DIFFERENT POSITIONS IN SUCH A WAY THAT EACH AXIS WAS ALIGNED WITH (+) OR AGAINST (-) GRAVITY: (A) Z+, (B) Z-, (C) X+, (D) X-, (E) Y, (F) Y-.....24

FIGURE 12: EXEMPLAR WIND ROSE DIAGRAM FOR STUDY DATES IN OCTOBER 2020. THE RED WEDGE OUTLINED ON THE WIND ROSE DIAGRAM INDICATES THE FREQUENCY OF WIND EVENTS REACHING SPEEDS (WS) BETWEEN 5-10KM/H FOR THE STUDY DATES IN OCTOBER.29

FIGURE 13: A SIMPLIFIED VERTICAL TRANSECT OF ESCARPMENT VEGETATION IN HAMILTON (NOT TO SCALE). PATTERNS OF PLANT GROWTH AND DEVELOPMENT CAN BE RELATED TO THE POSITION ON THE ESCARPMENT: UPPER PLATEAU, BEDROCK FACE, INTERMEDIARY PLATEAU (LEDGES), AND SLOPING TALUS (CREATED USING BIORENDER.COM)..31

FIGURE 14: A RIGHT-HAND COORDINATE SYSTEM SUPERIMPOSED ON THE AL101 TRIAXIAL ACCELEROMETER. EACH OF THE THREE AXES (X, Y, Z) ARE IDENTIFIED INCLUDING BOTH POSITIVE AND NEGATIVE PLANES. THE X-AXIS IS IN ALIGNMENT WITH THE GRAVITY VECTOR, INDICATED BY THE BLUE ARROW, IN THE VERTICAL POSITION.....35

FIGURE 15: THE RELATIONSHIP BETWEEN ACCELERATION ALONG THE Y- AND Z-AXES AND WIND SPEED FOR THE STUDIED DAYS IN THE MONTH OF OCTOBER, 2020. TREE BOLE TILT IS DEPICTED BY ACCELERATION(G) FOR UNIT B1(RED), UNIT B2 (YELLOW), AND UNIT R1(BLUE). WIND SPEED (KM/H) IS INDICATED BY THE DASHED GREY LINE. INCREASED TILT ALONG THE Y- AND Z-AXES ARE INDICATED BY INCREASING VALUES OF ACCELERATION(G). UNIT B2 (YELLOW) IS PLOT ON A SECONDARY Y-AXIS TO BETTER SHOW DIURNAL VARIATION OF TILT. DUE TO DISCREPANCIES IN THE ANGLE OF ACCELEROMETER PLACEMENT, A CORRECTION FACTOR HAS BEEN ADDED TO ORIGINAL ACCELERATION DATA FOR THE WHITE CEDAR (B2; YELLOW; SEE PAGE 43 FOR FURTHER EXPLANATION OF THIS CORRECTION).37

FIGURE 16: THE RELATIONSHIP BETWEEN ACCELERATION ALONG THE Y- AND Z-AXES AND WIND SPEED FOR THE STUDIED DAYS IN THE MONTH OF NOVEMBER. TREE BOLE TILT IS DEPICTED BY ACCELERATION(G) FOR UNIT B1(RED), UNIT B2 (YELLOW), AND UNIT R1(BLUE). WIND SPEED (KM/H) IS INDICATED BY THE DASHED GREY LINE. INCREASED TILT ALONG THE Y- AND Z-AXES ARE INDICATED BY INCREASING VALUES OF ACCELERATION(G). UNIT B2 (YELLOW) COVERS A SHORTER PERIOD OF TIME DUE TO AN ISSUE WITH BATTERY-LIFE. UNIT B2 (YELLOW) COVERS A SHORTER PERIOD OF TIME DUE TO AN ISSUE OF BATTERY-LIFE. UNIT B2 (YELLOW) IS PLOT ON A SECONDARY Y-AXIS TO BETTER SHOW DIURNAL VARIATION OF TILT. DUE TO DISCREPANCIES IN THE ANGLE OF ACCELEROMETER PLACEMENT, A CORRECTION FACTOR HAS BEEN ADDED TO ORIGINAL ACCELERATION DATA FOR THE WHITE CEDAR (B2; YELLOW; SEE PAGE 43 FOR FURTHER EXPLANATION OF THIS CORRECTION).38

FIGURE 17: THE RELATIONSHIP BETWEEN ACCELERATION ALONG THE Y- AND Z-AXES AND WIND SPEED FOR THE STUDIED DAYS IN THE MONTH OF MARCH. TREE BOLE TILT IS DEPICTED BY ACCELERATION(G) FOR UNIT B1(RED), UNIT B2 (YELLOW), AND UNIT R1(BLUE). WIND SPEED (KM/H) IS INDICATED BY THE DASHED GREY LINE. INCREASED TILT ALONG THE Y- AND Z-AXES ARE INDICATED BY INCREASING VALUES OF ACCELERATION(G). UNIT B1 (RED) COVERS A SHORTER PERIOD OF TIME DUE TO AN ISSUE OF BATTERY-LIFE. UNIT B2 (YELLOW) IS PLOT ON A SECONDARY Y-AXIS TO BETTER SHOW

DIURNAL VARIATION OF TILT. DUE TO DISCREPANCIES IN THE ANGLE OF ACCELEROMETER PLACEMENT, A CORRECTION FACTOR HAS BEEN ADDED TO ORIGINAL ACCELERATION DATA FOR THE WHITE CEDAR (B2; YELLOW; SEE PAGE 43 FOR FURTHER EXPLANATION OF THIS CORRECTION).39

FIGURE 18: THE RELATIONSHIP BETWEEN ACCELERATION ALONG THE Y- AND Z-AXES AND WIND SPEED FOR THE STUDIED DAYS IN THE MONTH OF MAY. TREE BOLE TILT IS DEPICTED BY ACCELERATION(G) FOR UNIT B1(RED), UNIT B2 (YELLOW), AND UNIT R1(BLUE). WIND SPEED (KM/H) IS INDICATED BY THE DASHED GREY LINE. INCREASED TILT ALONG THE Y- AND Z-AXES ARE INDICATED BY INCREASING VALUES OF ACCELERATION(G). UNIT R1 (RED) WAS PLOT ON A SECONDARY Y-AXIS TO BETTER SHOW DIURNAL VARIATION OF TILT. DUE TO DISCREPANCIES IN THE ANGLE OF ACCELEROMETER PLACEMENT, A CORRECTION FACTOR HAS BEEN ADDED TO ORIGINAL ACCELERATION DATA FOR THE WHITE CEDAR (B2; YELLOW) AND THE RED OAK (B1; RED; SEE PAGE 43 FOR FURTHER EXPLANATION OF THIS CORRECTION).40

FIGURE 19: WIND ROSE DIAGRAMS FOR STUDY DATES IN (A) OCTOBER, (B) NOVEMBER, (C) MARCH, AND (D) MAY. WIND DIRECTION IS DISPLAYED BY CARDINAL DIRECTION ON THE PERIMETER OF THE DIAGRAM, AND WIND SPEED (KM/H) IS REPRESENTED BY COLOUR. WIND SPEEDS WERE SUBDIVIDED INTO CATEGORIES, STARTING FROM 0 KM/H AND INCREASING AT INTERVALS OF 5 KM/H. EACH CONCENTRIC CIRCLE WITHIN THE ROSE CORRESPONDS TO THE FREQUENCY (%) OF WIND EVENTS FROM A CERTAIN DIRECTION AND SPEED CATEGORY. FREQUENCY IS INDICATED BY A PERCENTAGE AND VARY FOR EACH MONTH OF STUDY.45

FIGURE 20: BAR PLOT DEPICTING CHANGES IN MODIFIED CANOPY COVER (%) CALCULATED USING GLAMA. CANOPY COVER MEASUREMENTS WERE TAKEN FOR EACH OF THE FOUR MONTHS OF STUDY; MAY (BLUE), OCTOBER (ORANGE), NOVEMBER (YELLOW), AND MARCH (PURPLE). B1 (RED OAK), B2 (WHITE CEDAR), AND R1 (SUGAR MAPLE) STUDY SITES (FIGURES 21-23).47

FIGURE 21: (A) MOUNTED AL101 ON THE SUGAR MAPLE (R1) AND SURROUNDING FOREST STRUCTURE LOCATED ALONG THE CHEDOKE RADIAL TRAIL, (B) CANOPY VIEW OF THE SUGAR MAPLE (R1) AND OVERLYING CANOPY ARCHITECTURE, (C) MAP OF FIELDWORK LOCATIONS ALONG THE NIAGARA ESCARPMENT AND HIGHLIGHTING THE LOCATION OF THE SUGAR MAPLE (R1).48

FIGURE 22: (A) MOUNTED AL101 ON THE RED OAK (B1) AND SURROUNDING FOREST STRUCTURE LOCATED ALONG THE ROCKCLIFFE TRAIL, (B) CANOPY VIEW OF THE RED OAK (B1) AND OVERLYING CANOPY ARCHITECTURE, (C) MAP OF FIELDWORK LOCATIONS ALONG THE NIAGARA ESCARPMENT AND HIGHLIGHTING THE LOCATION OF THE RED OAK (B1).49

FIGURE 23: (A) MOUNTED AL101 ON THE WHITE CEDAR (B2) AND SURROUNDING FOREST STRUCTURE LOCATED ALONG THE ROCKCLIFFE TRAIL, (B) CANOPY VIEW OF THE WHITE CEDAR (B2) AND OVERLYING CANOPY ARCHITECTURE, (C) MAP OF FIELDWORK LOCATIONS ALONG THE NIAGARA ESCARPMENT AND HIGHLIGHTING THE LOCATION OF THE WHITE CEDAR (B2).50

FIGURE 24: (LEFT) A SIMPLIFIED VERTICAL TRANSECT OF ESCARPMENT VEGETATION IN HAMILTON (NOT TO SCALE). PATTERNS OF PLANT GROWTH AND DEVELOPMENT CAN BE RELATED TO THE POSITION ON THE ESCARPMENT: UPPER PLATEAU, BEDROCK FACE, INTERMEDIARY PLATEAU (LEDGES), AND SLOPING TALUS; (RIGHT) IDEAL DISTRIBUTION OF VEGETATION SPECIES SUITABLE FOR MITIGATING SLOPE EROSION ALONG DIFFERENT POSITIONS OF THE ESCARPMENT (CREATED USING BIORENDER.COM).55

FIGURE 25: MAIN FACTORS IMPACTING THE TREE BOLE TILT FOR DECIDUOUS SPECIES (LEFT) AND CONIFEROUS SPECIES (RIGHT) INVESTIGATED IN THIS STUDY. WIND DIRECTION WAS MOST STRONGLY CORRELATED TO TREE BOLE TILT OF DECIDUOUS TREES, WHEREAS WIND SPEED WAS MOST STRONGLY CORRELATED TO TILT ALONG THE BOLE OF THE

CONIFEROUS TREE. TILT WAS GENERALLY GREATEST AROUND MID-DAY, AND HAD THE STRONGEST IMPACT ON ALL MONITORED TREES DURING THE STUDY DATES IN NOVEMBER (CREATED USING BIORENDER.COM).....57

FIGURE 26: SCHEMATIC DIAGRAM SHOWING POTENTIAL ENVIRONMENTAL FACTORS IMPACTING EROSIONAL PROCESSES ON THE NIAGARA ESCARPMENT IN HAMILTON, WITH A PARTICULAR FOCUS ON VEGETATION GROWTH IN BEDROCK DISCONTINUITIES AND ASSOCIATED WEATHERING PROCESSES, AND TREE SWAY MOVEMENT DURING PERIODS OF WIND EXCITATION DOCUMENTED USING TRIAXIAL ACCELEROMETERS (CREATED USING BIORENDER.COM).....60

List of Tables

TABLE 1: OVERVIEW OF TREE SPECIES AND GEOSPATIAL CHARACTERISTICS RELATED TO THE THREE TREES USED IN THIS RESEARCH. EACH TREE IS IDENTIFIED BY A UNIT CODE ASSOCIATED WITH THE ACCELEROMETER MOUNTED TO THE TREE.	20
TABLE 2: LIST OF SPECIES AND CORRESPONDING POSITION ALONG THE TOPOGRAPHIC GRADIENT OF THE ESCARPMENT WITHIN HAMILTON.	33
TABLE 3: SUMMARY STATISTICS IDENTIFYING CORRELATIONS BETWEEN WIND SPEED AND ACCELERATION ALONG THE Y-AXIS FOR EACH MONTH OF STUDY FOR EACH TREE SPECIES EXAMINED IN THIS RESEARCH. CORRELATIONS WERE DETERMINED BY PERFORMING A PEARSON PRODUCT-MOMENT CORRELATION COEFFICIENT. P-VALUES < 0.05 ARE CONSIDERED STATISTICALLY SIGNIFICANT RESULTS.	44
TABLE 4: SUMMARY STATISTICS IDENTIFYING CORRELATIONS BETWEEN WIND DIRECTION AND ACCELERATION ALONG THE Y-AXIS FOR EACH MONTH OF STUDY AND EACH TREE SPECIES EXAMINED IN THIS RESEARCH. CORRELATIONS WERE DETERMINED BY PERFORMING A PEARSON PRODUCT-MOMENT CORRELATION COEFFICIENT. P-VALUES < 0.05 ARE CONSIDERED STATISTICALLY SIGNIFICANT RESULTS.	46

1. Introduction

The Niagara Escarpment is a striking geomorphological feature that extends over 700 kilometers from western New York State, through southern Ontario and Manitoulin Island, to the Upper Peninsula of Michigan, culminating in central Wisconsin (Brunton & Brintnell, 2020; Figures 1, 2). The escarpment is comprised of carbonate-dominated Paleozoic strata, exposing dolostone, sandstone, and shale deposits of Ordovician and Early Silurian age (Cox, & Larson, 1992). A combination of differential erosion processes, including glacial scouring during the Quaternary and postglacial streamflow, have formed the steep cliff faces of the escarpment. More erosion-resistant and highly fractured dolostone lithologies are undercut by softer shale strata leading to the creation of an unstable overhanging caprock, and overall recession of the escarpment face (Cox & Larson, 1992). Previous research on escarpment geomorphology has examined slope stability and its relationship with, and dependence on, environmental variables, and morphological characteristics related to lithology (Hewitt, 1971; Brett *et al.*, 1999; Barlow, 2002; Hayakawa & Matsukura, 2010; Brunton & Brintnell, 2021). Relatively few studies have focused on the relationship between erosion and overall ecosystem characteristics (Moss & Nickling, 1980; Cox & Larson, 1992; Parker & Bendix, 1996; Moss & Milne, 1998). The few studies that do, provide an initial analysis of the dynamic relationships between vegetation growth and active geomorphic processes on an exposed bedrock escarpment. However, these early approaches to slope stability assessment do not encompass symbiotic hydrologic and biologic relationships or allow for the prediction of areas prone to future slope failure (Moss & Nickling, 1980). Factors such as changes in precipitation and/or drainage patterns can compromise slope stability and exacerbate erosion of the scarp face through loss of stabilizing vegetation (HCA Planning and Regulations Polices, 2011). The geomorphology of the Niagara Escarpment is dynamic and continually changing, resulting in a need to strategically develop, modify, and protect the landscape in a manner which will account for future dynamic morphological changes.

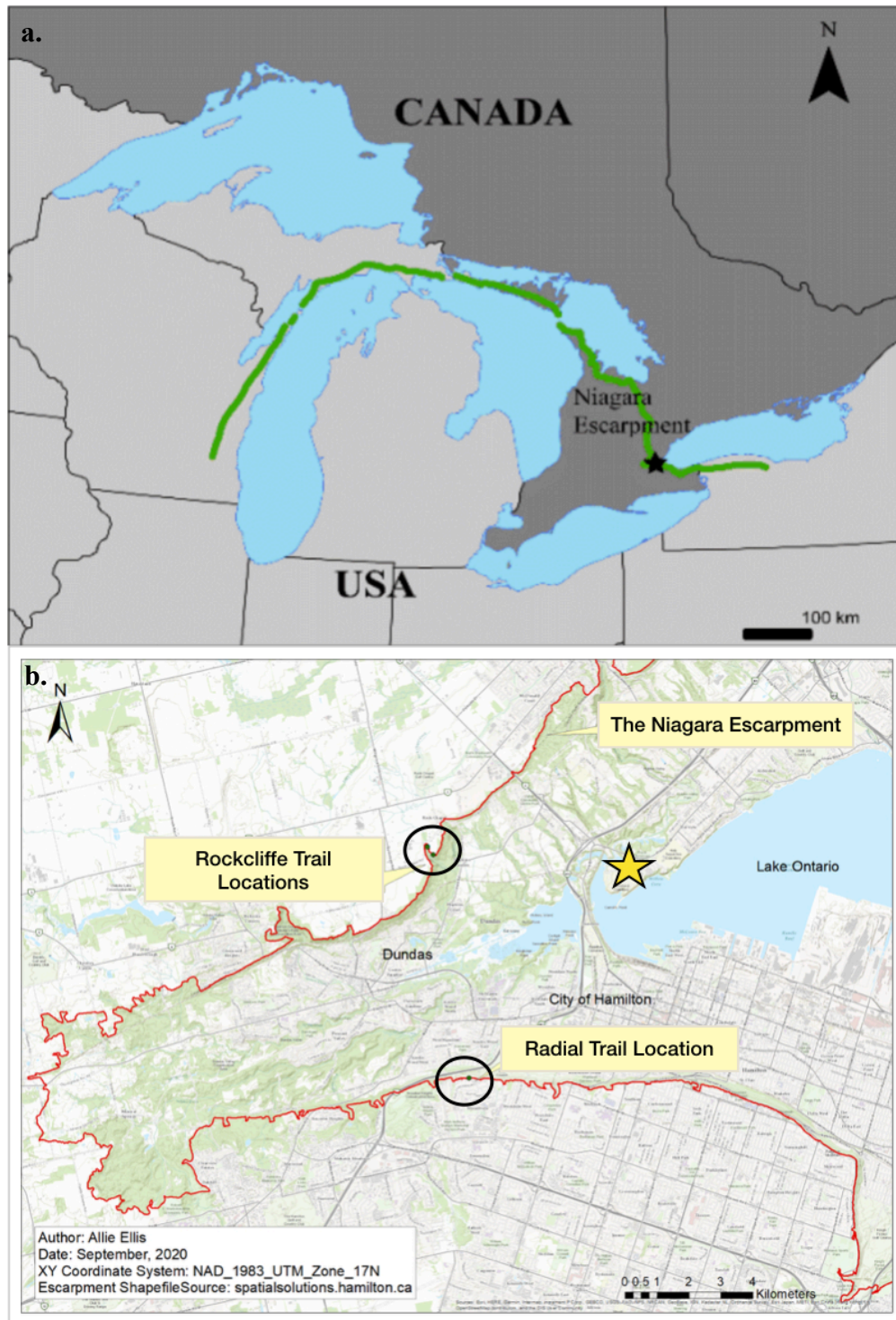


Figure 1: (a) Geographic extent of the Niagara Escarpment (green) within eastern North America. The escarpment extends from western New York State, through Ontario, Michigan, and central Wisconsin. The location of Hamilton, Ontario is indicated by a star (Lee, 2020). (b) Map depicting regional fieldwork locations (black circles) in the City of Hamilton and their position on the Niagara Escarpment (red outline). Green dots highlight the placement of accelerometer equipment - two at the Rockcliffe trail location and one at the Chedoke Radial Trail location; yellow star indicates the location of the Royal Botanical Gardens (RBG) Weather Station.

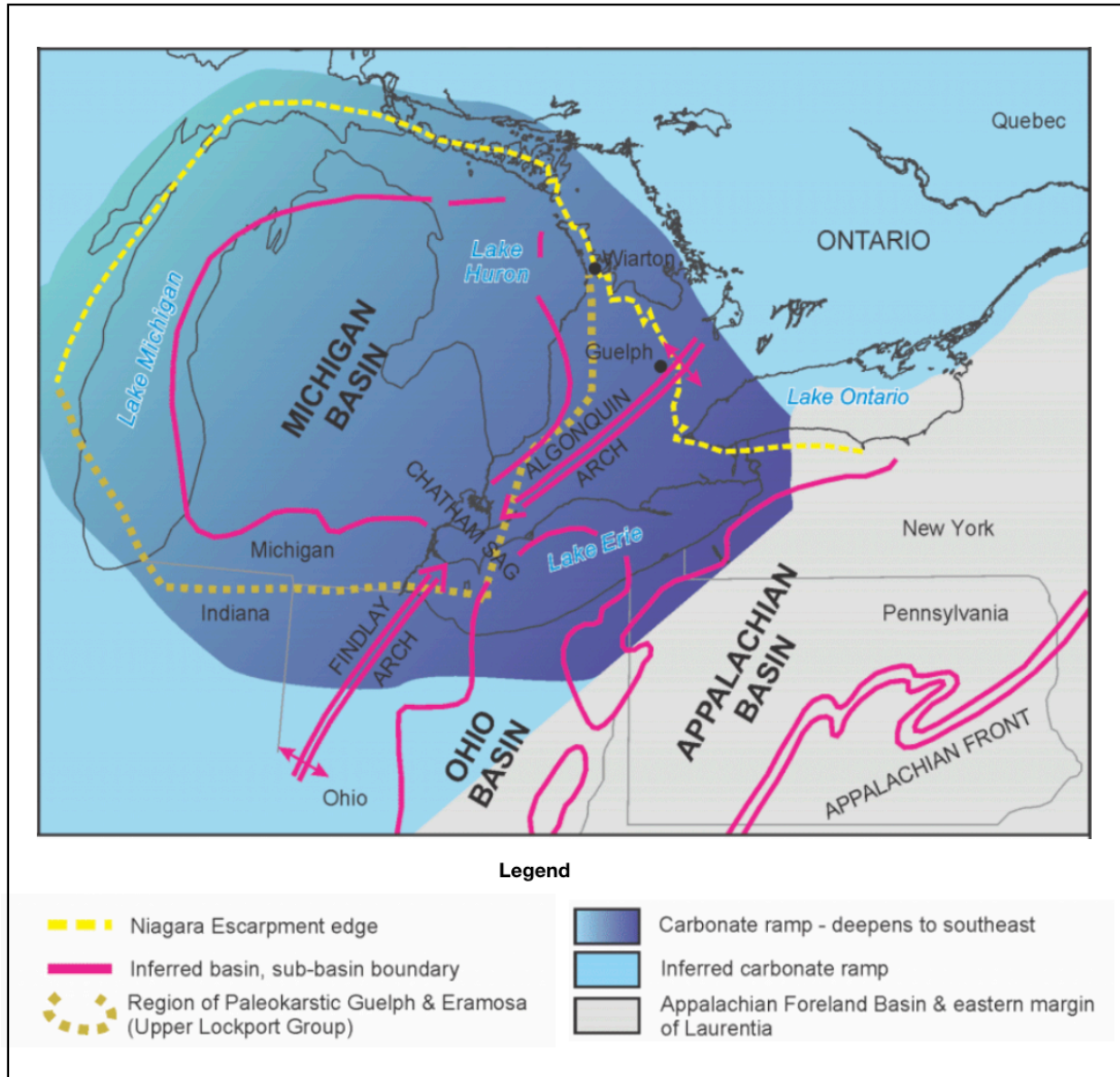


Figure 2: Early Silurian paleogeography relative to present-day erosional boundaries including the Appalachian foreland basin, Michigan intracratonic basin and the Algonquin-Findlay arches (indicated by the thick pink lines). The dashed yellow line represents the geographic extent of the Niagara Escarpment in relation to the basins, and sub-basin boundaries of the early Silurian paleogeography (Reproduced from Brunton & Brintnell, 2020, with permission).

Starting in the late 1950's, concerned citizen groups have lobbied for increased preservation and control on land use, planning, and development along the escarpment (Moss & Milne, 1998). In response to these calls, the Niagara Escarpment Planning and Development Act was passed in 1973, leading to the formation of the Niagara Escarpment Commission (NEC), a provincial government agency responsible for administering the Niagara Escarpment Plan (NEP), approved in 1985 (Moss & Milne, 1998).

The NEP is committed to maintaining the escarpment and its surrounding natural environment and to ensuring only developments compatible with natural ecosystem dynamics be pursued (Rodie & Post, 2009). By 1990, the escarpment was designated a World Biosphere Reserve by UNESCO and remains a protected area under the Province of Ontario's Niagara Escarpment Planning and Development Act (Rodie & Post, 2009). The Niagara Escarpment is now recognized as both a unique geomorphological landscape feature of local, provincial, national, and international importance, as well as a distinctive forested ecosystem.

The City of Hamilton is located within the Great Lakes Region of southern Ontario, Canada, and is bisected by the Niagara Escarpment (Figure 1). The stability of the escarpment face is a critical concern for Hamilton city planners as the increased frequency and severity of bedrock erosion and weathering has resulted in closures of important corridors connecting portions of the city above and below the escarpment (Figures 1, 3). Escarpment resource planning and management strategies to date have failed to effectively consider dynamic Earth system processes, in particular those related to vegetation growth, which contribute to landform evolution. Vegetation growth can contribute to both erosional and stabilization processes on steep, heavily jointed, bedrock outcrops. Root growth can exploit geologic structures through deployment into fractures, fissures, and bedding planes, and can also provide mechanical reinforcement on unstable slopes through root-binding actions. The lack of understanding of exactly how vegetation can physically weather bedrock and facilitate erosion of the Niagara Escarpment has led to the motivation for this study.



Figure 3: Access roadways cutting through the Niagara Escarpment in Hamilton and associated erosion of steep marginal slopes (a) top of the Jolley Cut roadway and view of lower downtown core, (b) small bedrock slide along the Jolley Cut, (c,d) failed infrastructure installed to prevent erosion along the Sherman Cut roadway (Lee, 2018).

1.1 Objectives

Most studies related to vegetation productivity have been confined to consideration of climate and topsoil features, whereas the importance of deeper subsurface components remain poorly understood (Richter & Billings, 2015, Jiang *et al.*, 2020). The aim of the research presented here is to identify and explore methods to quantify the impacts of vegetation on erosional processes along the Niagara Escarpment in Hamilton, Ontario and to investigate the interactions between vegetation and bedrock discontinuities. The specific objectives of this research are to (1) document slope characteristics and determine how this impacts vegetation growth and development, (2) monitor tree sway movement and responses to wind gusts and how the forces exerted by tree tilt may impact underlying bedrock, and (3) consider how characteristics of tree species affect the frequency and magnitude of wind-driven tree bole movements. The outcomes of this research can

be used to facilitate the design of effective vegetation management strategies on the Niagara Escarpment in Hamilton and can form an integral component of an erosion-risk assessment program.

1.2 Geological Setting

Three main geological features dominate the physiography of the Great Lakes Region of Southern Ontario: the Algonquin Arch, the Michigan Basin, and the Allegheny Basin, part of the larger Appalachian Basin (Barlow, 2002; Figure 2). The Algonquin Arch is a southwest-plunging anticline that forms the spine of southern Ontario and straddles the boundary between the Michigan intracratonic basin and Appalachian foreland basin (Tovell, 1992; Brunton & Brintnell, 2020). Northwest of the arch, in the area located between lakes Huron and Michigan, Phanerozoic sedimentary strata dip into the Michigan Basin; southeast of the arch, sedimentary strata overlying Precambrian basement dip into the Allegheny Basin (Tovell, 1992; Figure 2). Hence, lithological units lying north of Hamilton dip to the southwest into the Michigan Basin, while those located along the Niagara Peninsula and New York State dip gently to the south into the Allegheny Basin (Barlow, 2002). The escarpment reaches its highest elevation (546 m a.s.l) where it intersects the Algonquin Arch south of Collingwood, and at Hamilton, the escarpment has an average elevation of just 150 m a.s.l. (Barlow, 2002). The escarpment has migrated to its current position through progressive southwestward (down dip) erosion by glacial and fluvial processes during the late Cenozoic (Straw 1968; Tovell, 1992; Barlow, 2002). Structural weakness exploited by local drainage systems contribute to the irregularity of the escarpment and array of reentrant valleys along its length (Figure 1). The escarpment face continues to weather and erode through processes such as freeze-thaw, mass wasting, and dissolution processes that affect the exposed carbonate-rich lithologies.

1.3 Geology of the Niagara Escarpment in Hamilton

The stratigraphy and lithologic units exposed along of the Niagara Escarpment have been described at length in several previous works including those by Hewitt (1971), Armstrong & Dodge (2007), and more recently, by Brunton & Brintnell (2020). The analysis presented in this

study focuses on lithological units that belong to the upper Lockport and Clinton Groups as these units form the caprock to the escarpment in Hamilton and experience the highest frequency of erosional events (Figures 3 and 4). Brief descriptions of the lithological units examined in this study and their structural characteristics are provided below.

The Lockport Group exposed along the Niagara Escarpment within the city of Hamilton is comprised of two prominent members: the Ancaster Member of the Goat Island Formation and the underlying Gasport Formation (Figure 4). The uppermost Ancaster Member of the Goat Island Formation is comprised of thin to medium bedded argillaceous dolostone with abundant chert nodules and irregular fractures (Brunton & Brintnell, 2020). The highly fractured and unstable nature of the Ancaster and its topmost position along the escarpment in Hamilton, directly impacts the stability of the escarpment caprock. Significant rockfalls resulting from the instability of the Ancaster Member have contributed to numerous road closures (Van Dongen, 2016; Mitchell, 2022) and threaten future escarpment stability. The Gasport Formation underlies the Goat Island and is a massive to crudely bedded, blue grey dolostone (Hewitt, 1971). This unit is more thickly bedded and is less intensely fractured than the overlying Ancaster Member (Figure 4).

The Clinton Group underlies the Lockport and consists of the Rochester Formation comprised primarily of shale with interbedded limestone, the dolomitic Irondequoit Formation, and the Reynales Formation (Figure 4). The easily eroded shales of the Rochester allow undercutting of the overlying, more erosion-resistant dolostones of the Lockport Group and contribute substantially to instability of the escarpment face (Hewitt, 1997; Moss & Milne, 1998). The underlying Irondequoit Formation is a bioturbated, vuggy, massive dolostone that possesses a relatively consistent thickness of approximately 1-1.5 meters throughout the study area in Hamilton. The Reynales Formation consists of fine to medium grained, crystalline light-grey dolomite with thin, grey shale interbeds. The basal sections of the Niagara Escarpment expose deposits of the Medina Group, dominated by interbedded sandstones and shales with minor dolostone (Figure 4).

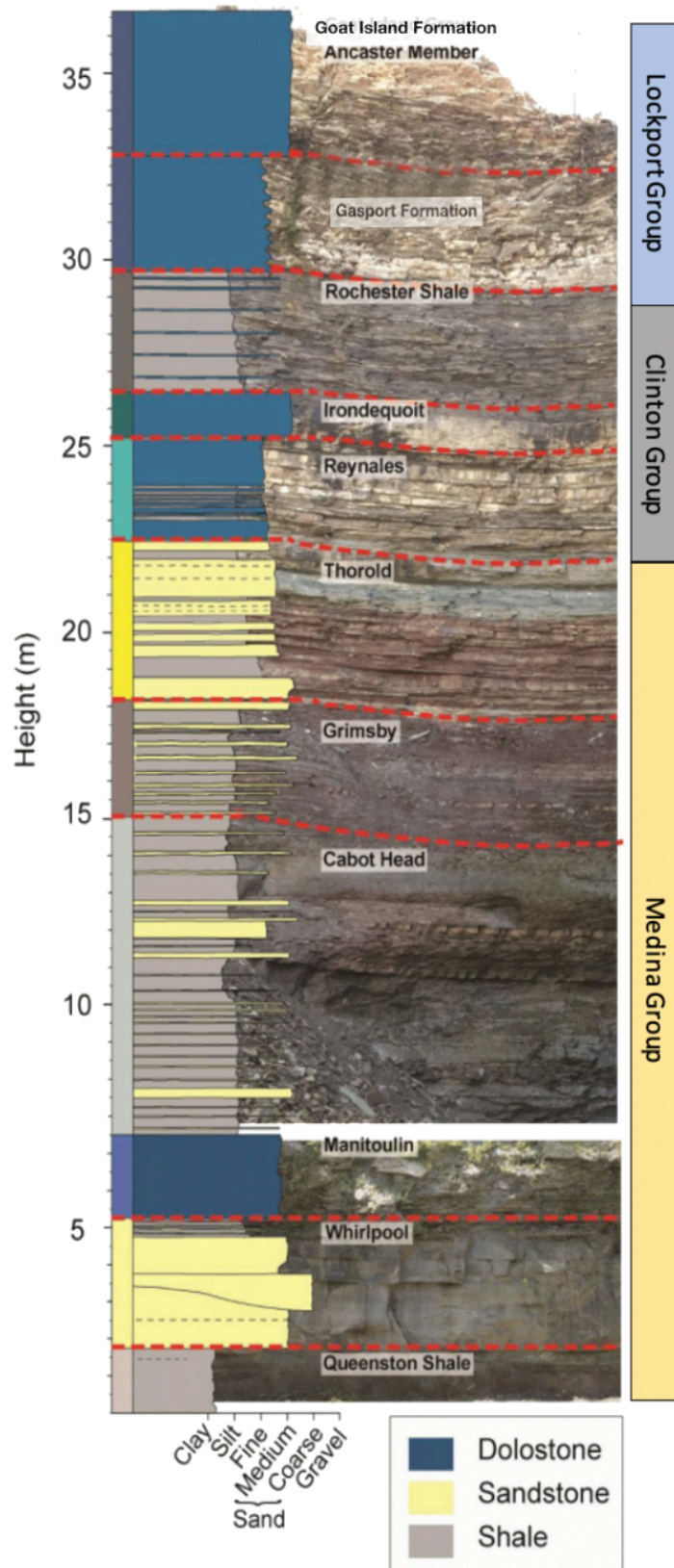


Figure 4: The major stratigraphic groups, and formations exposed along the Niagara Escarpment in Hamilton, Ontario (Lee, 2022.)

1.4 Vegetation Characteristics of the Niagara Escarpment in Hamilton

The city of Hamilton is located within the Lake Erie-Lake Ontario Ecoregion, also known as the Southern Deciduous Forest Region or Canadian Carolinian Forest Region (Crins *et al.*, 2009; Dickinson & Royer, 2021; Figure 5). This area of southern Ontario lies along the shores of Lake Erie and Lake Ontario and contains more than 25% of Canada's vascular plant species (Dickinson & Royer, 2021). Most of this ecoregion has now been converted to urban areas or cropland to support growing populations in the Greater Toronto Area. Remaining forests are defined as dense deciduous or mixed forests, and characterized by sugar maple (*Acer saccharum*), American beech (*Fagus grandifolia*), white oak (*Quercus alba*), (northern) red oak (*Quercus rubra*), and white ash (*Fraxinus americana*) (Crins *et al.*, 2009). In addition to deciduous forests, this ecoregion also supports the largest remnants of tall-grass prairie in the province (Crins *et al.*, 2009).

Vegetation growth on the Niagara Escarpment in Hamilton can be divided into three relatively distinct biophysical zones: the upper plateau, cliff face, and sloping talus (Cox & Larson, 1992; Figure 6). The geomorphological characteristics of the escarpment within each zone influences species richness and growth positions. Although species variability occurs between sites along the escarpment and among transects at each site, variations in vegetation and morphology at these scales are minor in comparison to the upward gradient crossing the escarpment face. The transition from upper plateau to bedrock face to sloping talus occurs over a short distance and is characterized by pronounced changes in ecosystem dynamics, in a similar way to changes in plant communities identified along the escarpment by Larson *et al.* (1989) (Figure 6). Several environmental factors may contribute to this variability including aspect, soil accumulation, bedrock lithological characteristics, and physical disturbances imposed by natural causes and human activity.



Figure 5: The province of Ontario, Canada showing the three ecozones (upper: Hudson Bay Lowlands, Ontario Shield, Mixedwood Plains), and the three main ecoregions in southern Ontario (lower) indicated by colour and letter/number codes. The yellow star indicates the location of Hamilton, Ontario within the Lake Erie-Lake Ontario Ecoregion (Adapted from the Ecological Land Classification Primer, (2007) by ontario.ca).

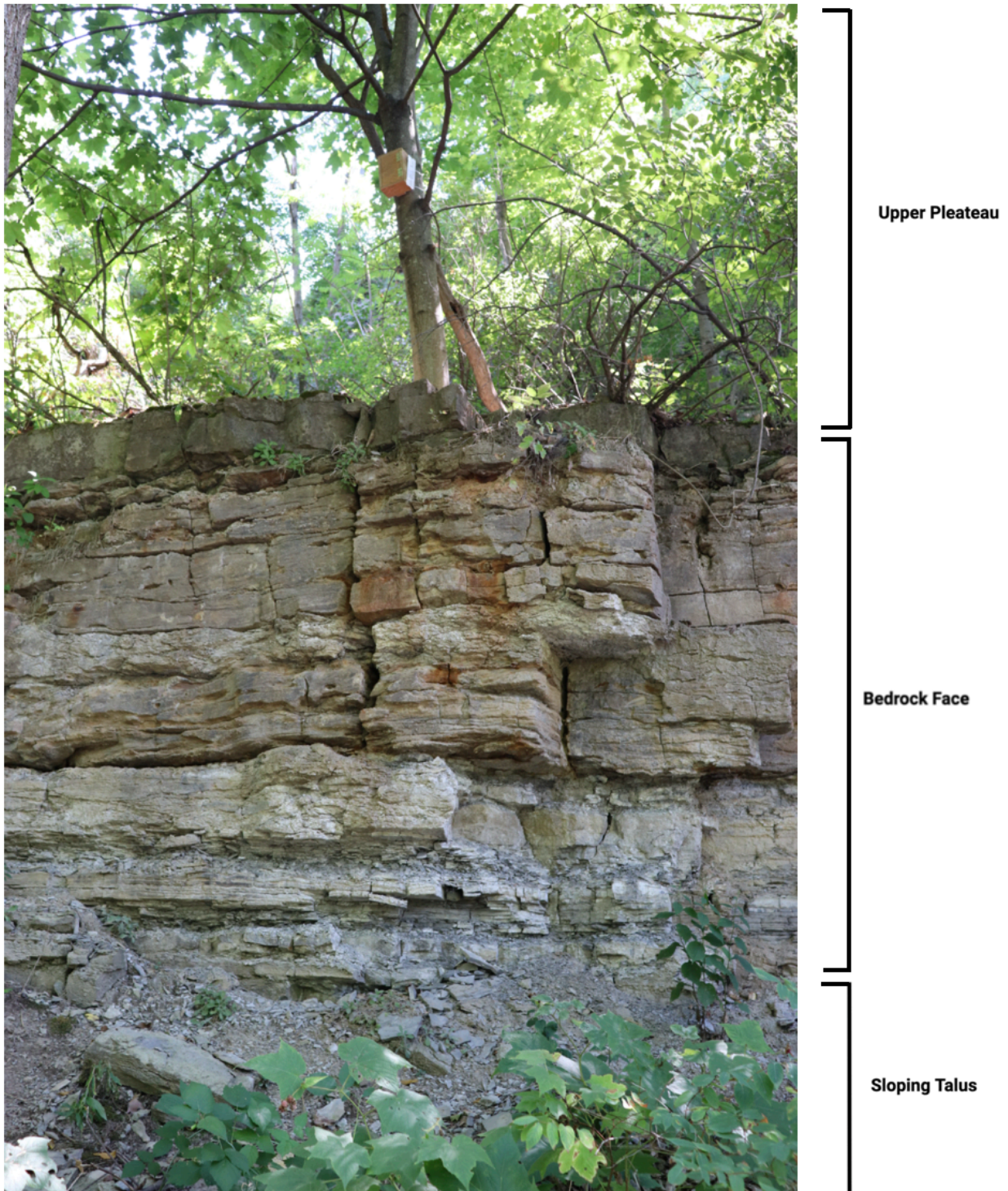


Figure 6: Vertical transect of escarpment vegetation in along the Chedoke Radial Trail, Hamilton. Patterns of plant growth and development can be related to the position on the escarpment: upper plateau, bedrock face, and sloping talus.

2. Vegetation and Slope Erosion

Physical weathering of exposed bedrock can occur as a result of a variety of processes including thermal expansion, frost cracking, and plant root growth. Through these processes, the properties of the rock such as strength, porosity, and hydraulic conductivity are altered and affect the potential for bedrock disaggregation (Anderson, 2019). Landforms exert a strong control on vegetation type and distribution, and vegetation in turn can function as a regulator of landform evolution. Hillslope stability can be modified by vegetation through root binding actions, rainfall interception, soil matric suction, weather events, and seasonal physiological changes (Hayati *et al.*, 2018). Early research on the role of plants in geomorphic and soil production processes has succinctly described plant rooting system influences on hillslope stabilization and the limitation of mass-wasting and erosion processes (Moss & Milne, 1998; Quine & Gardiner, 2007; Pawlik *et al.*, 2016). However, when accounting for biomechanical processes such as tree uprooting and bedrock disaggregation, the overall picture becomes more complex. Shallow soil profiles constrain vertical root growth, but the presence of cracks and fissures in underlying bedrock allows penetration by roots (Nie *et al.*, 2017). Tree roots have substantial impact on bedrock weathering and the formation of regolith, through biophysical and/or biochemical processes that alter bedrock surfaces particularly in cracks and fractures (Moses, Robinson, & Barlow, 2014).

Previous research has demonstrated that plant roots reinforce the soil profile mechanically on hillslopes (Wang *et al.*, 2005; Norris *et al.*, 2008). Root system architecture is important when considering the transfer of forces from the tree bole into the ground; the shape of the root system contributes to the mechanism by which these dynamic forces are distributed (Norris *et al.*, 2008). Heart-shaped rooting systems are considered to be the ideal configuration for reinforcing soils against slope instability as they are characterized by both oblique and laterally extending growth, and vertical shoots (Norris *et al.*, 2008).

Vegetation growing on sloped topography can also moderate ground stability through hydrological and mechanical processes. Canopy architecture regulates precipitation throughfall and root structures moderate the soil-water balance through biochemical and mechanical processes (Ghestem, Sidle, & Stokes, 2011). Planting native plant species is a useful strategy to mitigate many erosional processes and mass wasting events (Enns *et al.*, 2002). However, it is also possible that vegetation growth can disrupt underlying bedrock and enhance erosion processes. While

groundcover plants appear to be helpful in reducing erosional processes on soil covered slopes, the same may not be said for steep slopes underlain by highly fractured bedrock. Large, mature tree roots can easily penetrate bedrock fractures and appear to remain intact even after failure of the bedrock in which the roots had originally grown (Figure 7). While this may not mean that root growth was the catalyst for bedrock disaggregation and failure, it does indicate that vegetation growth on bedrock slopes has a different effect to that on soil covered slopes (Phillips, Turkington, & Marion, 2007; Pawlik *et al.*, 2016; Malik *et al.*, 2019).



Figure 7: Vegetation growing on bedrock along the Niagara Escarpment in Hamilton: (a) large roots of a mature tree remain intact after failure of highly-fractured underlying bedrock, (b) collapse of fractured bedrock blocks beneath an overlying soil and vegetation layer, (c) growth position of an established tree on the escarpment face. Red arrows highlight areas of previous bedrock erosion, evident by the spatial gaps between tree roots and the underlying surface.

2.1 Root Growth in Fractured Bedrock

Several studies have investigated the physical processes involved in the growth of tree roots in fractured bedrock (e.g. Nie *et al.*, 2017; Malik *et al.*, 2019). While these studies provide increased insight into the behavior of roots growing in rock, the question of whether tree roots are capable of biomechanically eroding unweathered bedrock surfaces remains uncertain. However, we do know that the maximum radial pressures exerted through root growth (0.51-0.9MPa) is a fraction of the average tensile strength of bedrock (1-25MPa), suggesting that radial root growth alone cannot cause mechanical disaggregation of bedrock (Malik *et al.*, 2019). However, biomechanical expansion of discontinuities in bedrock through root growth can operate in conjunction with other environmental factors, resulting in the enhanced weathering of bedrock and the widening of cracks (Malik *et al.*, 2019; Pawlik *et al.*, 2016).

If root growth and expansion alone cannot account for enhanced bedrock erosion rates, other mechanisms related to the growth of arboreal vegetation on steep bedrock slopes must be examined. Tree limbs, roots, and stems are subject to lateral movement in high winds, and extreme weather events can result in tree uprooting or stem breakage. However, lower wind speeds have also been shown to greatly impact stand structure and tree growth (Rudnicki, *et al.*, 2001). Exposure to chronic wind stress can result in plastic deformation of tree boles, branches, and wood cells. Under certain conditions of long-term stress, strong prevailing winds disturb natural tree growth, resulting in a windswept form in which branches and stem curve away from the wind (Moore, Gardiner, & Sellier, 2018). Tree throw, or stem breakage, occurs instantaneously, but the conditions leading up to these events may unfold over a much longer period of time.

There is substantial temporal and geographic variability in wind patterns experienced within a forest stand, from gusts lasting seconds to long-term seasonal weather patterns. The strength of wind in a single event is predominantly influenced by tree location relative to the storm center and ground topography. The aspect of hillslopes and orientation of valleys have considerable influence on the magnitude of wind speed experienced within a forest stand (Moore, Gardiner, & Sellier, 2018). In complex terrain, topography can alter the wind speed and direction significantly, with wind accelerating over hilltops and conversely funneling into valleys. Surface roughness, caused by factors such as irregular topography, buildings, or trees, may reduce mean wind speed but can also induce turbulence and gustiness, a catalyst for stem-breakage (Quine & Gardiner, 2007). In

addition, wind loading can vary due to the relative position of a tree within a stand, and its proximity to stand edges (Gardiner *et al.* 1997; Quine & Gardiner, 2007).

Seasonal physiological changes have also been found to have an impact on tree sway in broadleaved forests, although there is much debate about the impact of leaf loss during the winter season (Gardiner, 1992; Quine & Gardiner, 2007). In dense deciduous forests, leaf loss may increase wind penetration within the forest canopy and increase loading, while in mixed deciduous/coniferous forests, drag forces may increase on conifer trees during the winter months due to year-long canopy coverage. The increase of applied wind forces may overcome tree stem strength, resulting in wind throw, or cause the root plate to become unanchored resulting in tree overturn (Quine & Gardiner, 2007).

In addition to physical weathering processes, chemical weathering in the critical zone also contributes to bedrock disaggregation. Biomechanical interactions between tree roots and bedrock are obvious and common along the Niagara Escarpment where root growth encounters discontinuities in the bedrock (Figure 7). Previous work on escarpment vegetation by Matthes-Sears & Larson (1995), found that *Thuja occidentalis* (ancient white cedar) could grow their root systems entirely within fractured bedrock or with only limited access to soil. Rock weathering processes are enhanced through vegetation growth but are controlled by bedrock composition and physical features. Biochemical weathering is proliferated once plant roots have entered a discontinuity by moisture fluxes along the root (e.g. transpiration) and rhizosphere processes (e.g. mycorrhizal fungi). Mycorrhizal fungi are networks of branching fungi that not only penetrate surrounding soil and bedrock, but also extend into host plants forming a symbiotic relationship. Fungi can provide nutrients and water to host species and acquire carbohydrates from plant photosynthesis. Tree roots and associated mycorrhizal networks in the rhizosphere regulate the depth and rate of bedrock weathering through chemical processes that transport assimilated carbon to belowground biomass where microbes release CO₂ and organic acids (Brantley *et al.* 2011). The release of organic acid creates acidic water capable of dissolving minerals in rocks, opening pore spaces in the bedrock, and enhancing disaggregation processes (Schwinning, 2020). While the physical force that tree root growth exerts on bedrock likely does not play a significant role on the rate of bedrock disaggregation, the combination of both mechanical and chemical weathering mechanisms may result in increased bedrock fracturing in the presence of tree roots.

Little is currently known about the controls on root propagation into bedrock discontinuities and how tree-driven processes, such as sway, impact root infiltration and erosion (Brantley *et al.*, 2017). Progress is limited by a lack of direct force measurements exerted by trees and their roots in underlying bedrock. Several studies have investigated the tree-wind relationship using a variety of instruments and technologies including tilt sensors (Sellier *et al.*, 2003; Rudnicki *et al.*, 2001), videography (Peltola, 1996), strain gauges (Moore *et al.*, 2005), and accelerometers (Peltola, 1996; van Emmerik *et al.*, 2017). More recent advancements in technology and scientific instrumentation provide an opportunity to better monitor processes at the root-rock interface. Data logging triaxial accelerometers constitute a robust method for recording measurements of tree sway to quantify mechanisms that may influence bedrock weathering under chronic and acute weather events. An examination of past research outcomes related to the motion of trees in wind was synthesised by Jackson *et al.* (2021) where data from 20 studies and three different types of monitoring sensors, including accelerometers, were collated for review. Among their findings, Jackson *et al.* (2020) confirmed that the frequency at which a tree sways is strongly correlated to the size of the tree, and that coniferous forests exhibited distinct differences in sway responses to those of deciduous forests. However, many questions remain, such as how tree bole tilt is related to wind speed or direction? how tree properties impact damping mechanisms and dissipation of wind forces? and how plant growth may be linked to erosional processes? These remaining questions on how trees can affect the mechanical disaggregation of bedrock are of critical importance when examining escarpment bedrock erosion in the city of Hamilton.

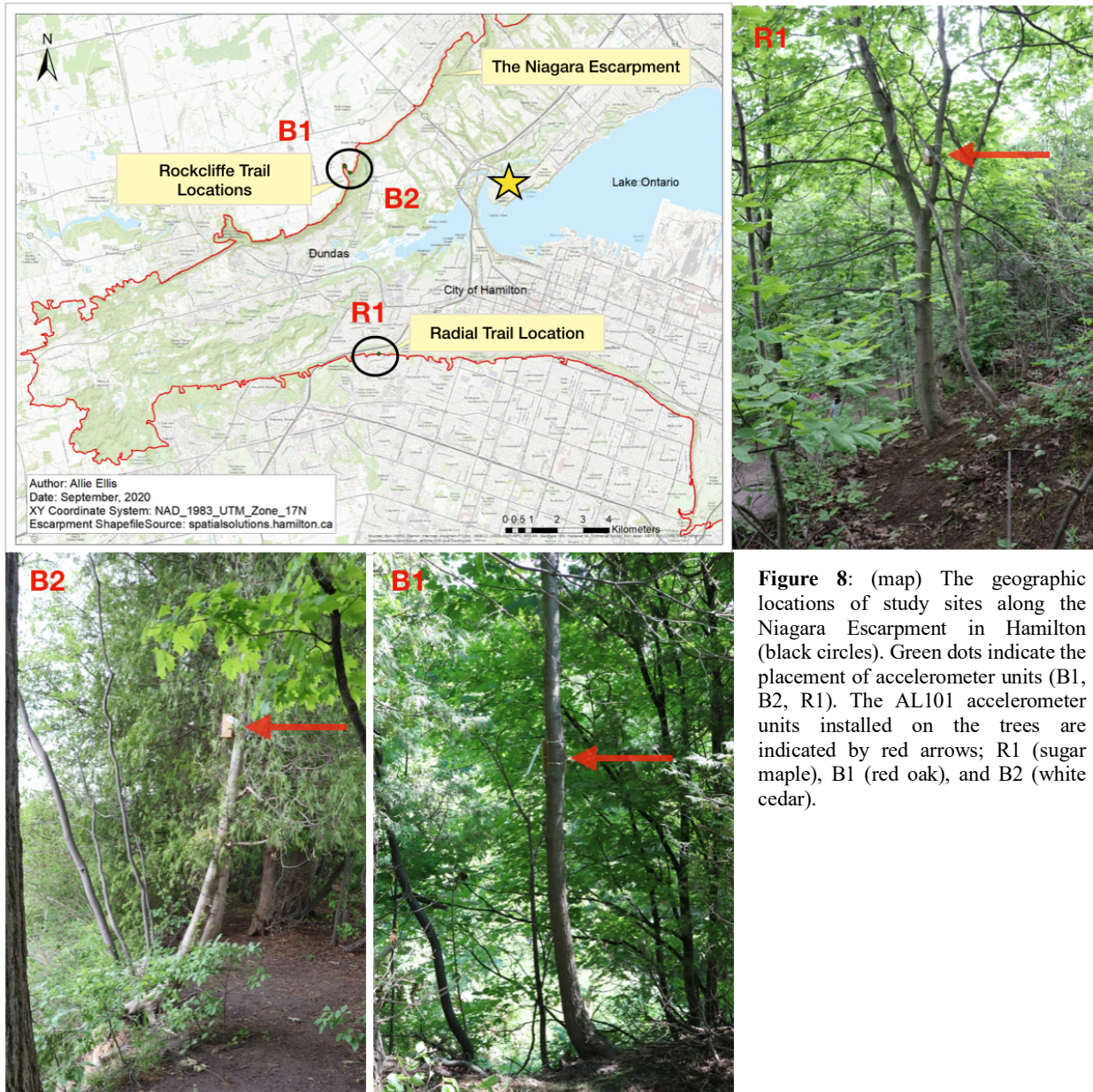
3. Study Design

3.1 Methods

3.1.1 Vegetation Survey

This study catalogued plant species, particularly trees and shrubs, at two selected study sites, Chedoke Radial Trail, and Rockcliffe Trail on the Niagara Escarpment (Figure 8). At both sites, vegetation growing on lithological units belonging to the Lockport and Clinton Groups was recorded using representative horizontal transects 6-8 meters in length. These lithological units

were chosen for detailed examination as they form the uppermost parts of the escarpment and are particularly prone to failure events. At each study site vegetation species, soil coverage, and aspect were documented together with GPS coordinates and elevation. Vegetation species were identified in the field using the phone application LeafSnap©Appixi and later confirmed using a vegetation guidebook (Dickinson & Royer, 2021). Approximate measurements of species density and frequency were recorded along with additional biotic features related to recent debris movement and evidence of vegetation recovery after erosional events. A standard vegetation inventory, using quadratic inventory methods, was not performed as general descriptions were deemed suitable to meet the needs of the research outcomes which focus on the effects of tree growth on the erosional stability of the Niagara Escarpment.



3.1.2 Tree Sway Measurement

To quantify the amount of tree sway occurring during the study period and evaluate its potential to affect bedrock, Acceleration Data Loggers (ORE - AL101) were mounted on three vertical tree trunks situated on the upper escarpment plateau, near the escarpment edge at the Radial Trail and Rockcliffe Trail study locations (Figure 8). Several studies have employed the use of accelerometers to measure tree sway and tilt in response to wind loads (van Emmerik *et al.*, 2017;

James *et al.*, 2013; Hassinen *et al.*, 1998; Peltola, 1996). Trees were chosen based on several criteria including species and maturity, accessibility and location, and underlying bedrock characteristics. Previous research indicates that the response to wind loading is different for conifers and deciduous trees and is strongly related to canopy architecture (Jackson *et al.*, 2021). To account for variability in canopy architecture, three trees of differing species (sugar maple, red oak, and white cedar) were chosen for an in-depth examination of the relationship between tree growth on fractured bedrock and tree sway (Table 1). Selected trees varied by species type and stage within the forest canopy, although quantitative dating of tree age was not possible. While all selected trees were growing on similar fractured dolostone bedrock, the erosional landscape and aspect of the escarpment did vary for each location (Table 1). The importance of walkability and access to equipment was also important for conducting safe field research practices.

Table 1: Overview of tree species and site characteristics related to the three trees used in this research. Each tree is identified by a Unit code associated with the accelerometer mounted to the tree.

Unit	Species		Location	Aspect	Formation	Lithology	DBH (cm)	Height (m)
	Botanical Name	Common Name						
R1	<i>Acer saccharum</i>	Sugar maple	Chedoke Radial Trail	N	Gasport	Dolostone	18.5	4.3
B1	<i>Quercus rubra</i>	Red oak	Rockcliffe Trail	NW	Goat Island	Dolostone	12.2	3.3
B2	<i>Thuja occidentalis</i>	White cedar	Rockcliffe Trail	SW	Goat Island	Dolostone	13.5	4.8

The AL101 is described by the manufacturer as “a general purpose triaxial acceleration logger designed to record the sway movement of trees” (ORE, 2021). Data collection using the AL101 commenced September 18, 2020 and was completed on May 27, 2021. Units were removed during the coldest months of the winter season (December to February) due to seasonal trail closures. Acceleration was recorded in three-dimensions (x, y, z), and continuously sampled at 100Hz/100Hz, or one sample/second. Battery-life limited tree monitoring to approximately 4-6 continuous days for each month of data collection. The accelerometer internal circuit board sits within an enclosure made of polycarbonate, designed for UV stabilization and weather protection (14.5cm long by 9.14cm wide by 5.5cm high) (Figure 9). Data were stored in 24h ASCII text files and later converted to Excel Workbooks for calibration. Units were attached to tree boles at least

two meters above the root-base (Figure 8); bole diameter at breast height (DBH) was measured using a standard measuring tape and tree height (m) using the mobile phone application Object Height for each tree studied.

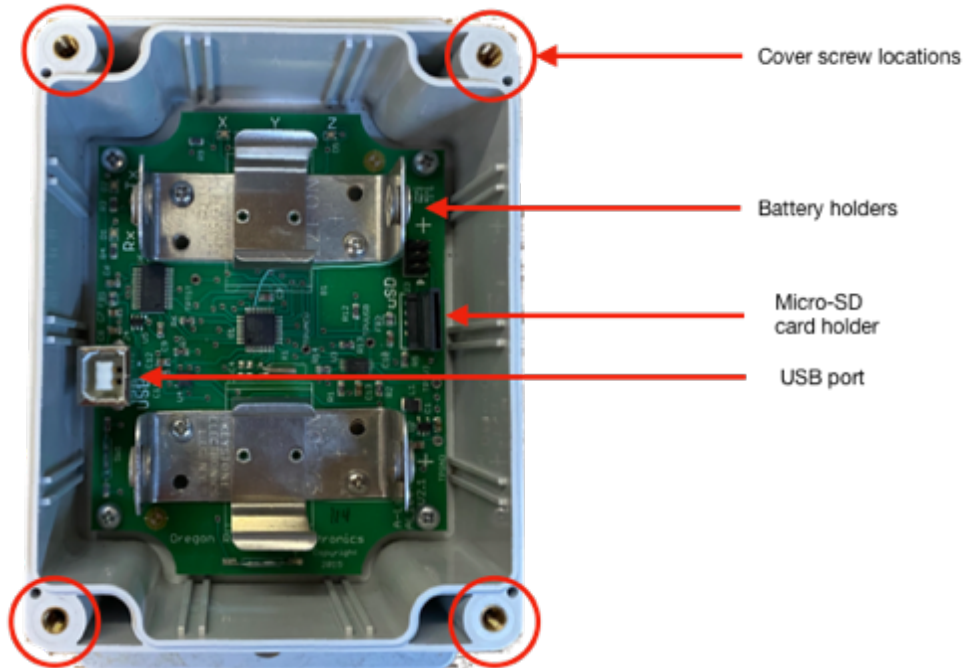


Figure 9: Internal circuit board of the AL101 accelerometer manufactured by Oregon Research Electronics (ORE). The battery holders, micro-SD holder, and USB port are indicated by red arrows, and cover screw locations are circled along the perimeter of the container.

3.1.3 Wind Data

To determine the relationship between wind strength and tree sway for the studied trees, wind speed and cardinal wind direction data were obtained from the Royal Botanical Gardens (RBG) Weather Station in Hamilton, Ontario (Figure 1B). Weather station equipment was not installed at the field sites due to (1) the potential for data interference and theft due to high levels of civilian traffic, (2) the impacts of escarpment slope and forest canopy on signal obstruction, and (3) variability in atmospheric conditions generated by the escarpment leading to inconsistent reporting between the two study locations. A recognized limitation of this study is the potential disparity

between wind speed and direction recorded at the RBG Weather Station and at the accelerometer monitoring sites.

3.1.4 *Canopy Survey*

The potential impact of seasonal canopy changes on tree sway motion was also considered in this study. Seasonal changes to canopy architecture are thought to have greater impact on deciduous dominant forests, but in mixed deciduous/coniferous forests, loss of leaves may increase drag on the conifer component during the winter season (Quine & Gardiner, 2007). Therefore, seasonal winter leaf-loss may result in a significant period of enhanced tree sway in Hamilton forests. Canopy openness was monitored at each of the study sites using the Gap Light Analysis Mobile Application (GLAMA) which utilizes hemispherical photographs of the overlying canopy to determine values of canopy closure (%) and canopy openness (%) (Jackson *et al.*, 2021; Quine & Gardiner, 2007).

3.2 Accelerometer Sensor Calibration

3.2.1 *Field Calibration*

Accelerometer units were calibrated prior to installation in the field using an ORE developed serial communications program called “AccelTerm”. The date and time were set at the beginning of each field deployment date, an automatic start after time delay was set to 10 minutes to omit movement caused during the installation period, and a sample rate of 100Hz/100Hz was programmed. A sample rate equal to one sample/second was chosen as this was considered to be adequate to record tree sway responses to wind loading. This rate was also chosen to limit the amount of data collected during the field experiment and to extend battery-life. Battery-life was inconsistent for all accelerometers across the study period and affected the duration of recordings. In November, unit B2 recorded approximately 24hrs less than units B1 and R1 due to battery failure, and in March, unit B1 recorded approximately 12hrs less than units B2 and R1.

It was important for the accelerometers to be in the same orientation after replacing batteries in each unit to accurately monitor changes in tree sway over the study period. To account for this,

wooden housing containers were built for storing each accelerometer while in the field (Figure 10). Wooden rails along the inside of the container allowed the accelerometer to slide in and out easily for battery replacement, and a rubber mount was adhered to the back of the container to limit agitation and destruction of underlying tree bark. The accelerometer container was strapped to the tree trunk using both metal and plastic zip-ties to maintain mounting height and angle of placement and left on for the duration of the experiment. While the housing containers may have maintained the orientation of the accelerometer throughout the experiment, the housing also increased the distance between monitoring equipment and the tree trunk. This may have impacted data collection and the ability for the accelerometer to monitor sway motions accurately but was necessary to protect the accelerometer and reduce visibility to passersby.



Figure 10: (a) Wooden housing container mounted to a tree bole with white plastic zip ties and sealed with a smaller, black zip tie during a trial of research equipment, (b) interior view of wooden housing container and the position of the AL101 during field research, (c) wooden housing container and AL101 installed at the Chedoke Radial Trail field site on a sugar maple (*Acer saccharum*) ~2.7m from the root base. The red circle indicates the location of the AL101 and wooden housing container.

3.2.2 Accelerometer Offset Calibration

The sensor output of the AL101 is un-normalized and recorded as 32 bits signed text characters. A sign character is added for negative values only. Text characters were computed to acceleration units of gravity (g) and calibrated to mitigate offset for further analysis.

Acceleration offset is defined as the reading reported by the monitoring equipment indicating acceleration when there should be zero acceleration. There are two common sources of offset including (1) internal machine generated offset, and (2) misalignment of AL101 with respect to the gravity vector. All accelerometers were rotated through the six canonical orientations (Figure 11) to account for machine generated offset with respect to the gravity vector. The accelerometers

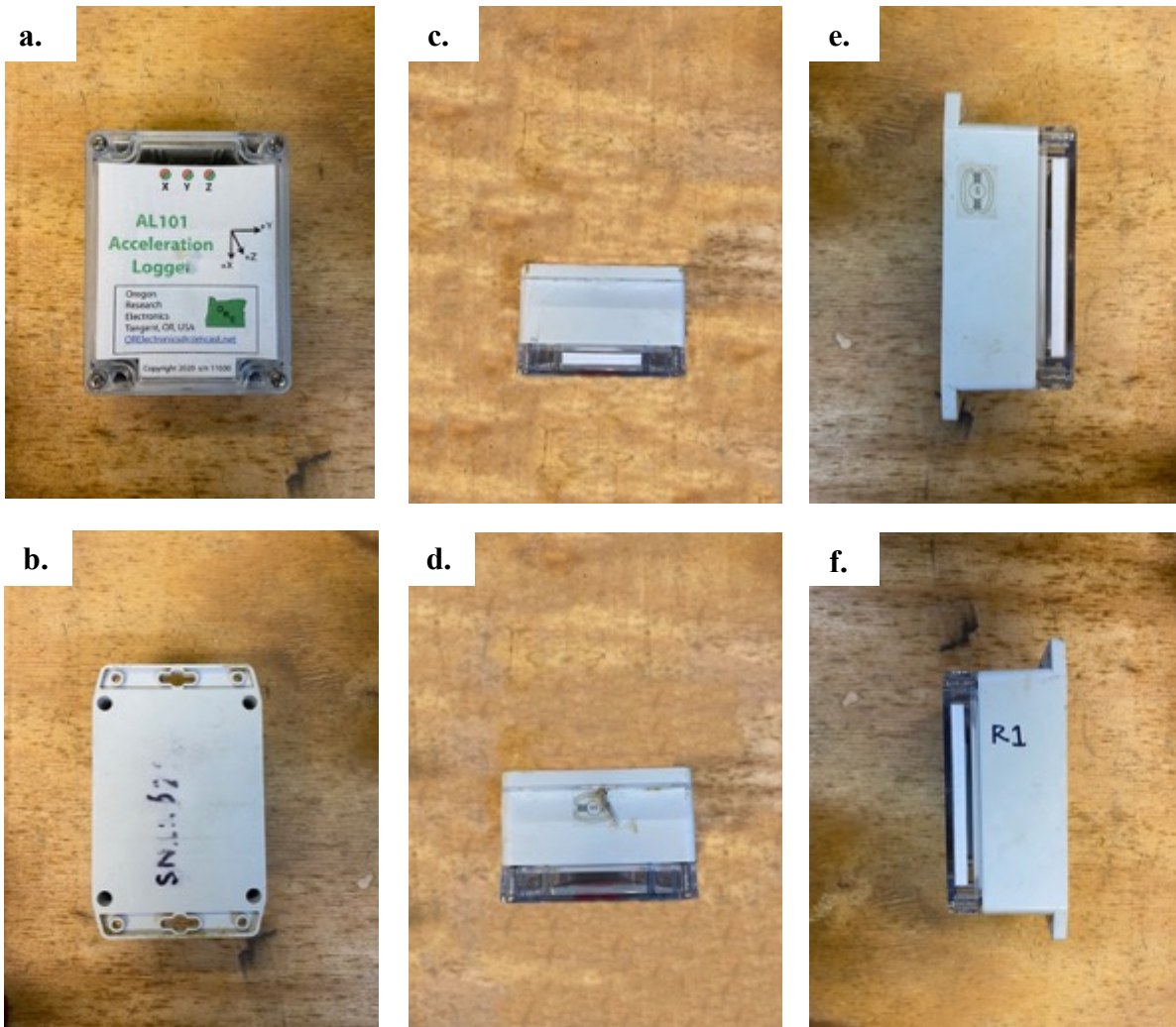


Figure 11: Accelerometer R1 in the six canonical positions used to calculate offset for each axis (X, Y, Z). The accelerometer was rotated through different positions in such a way that each axis was aligned with (+) or against (-) gravity: (a) Z+, (b) Z-, (c) X+, (d) X-, (e) Y, (f) Y-.

were calibrated in a temperature stable room ($\sim 20^{\circ}\text{C}$) and remained in each canonical position for ~ 35 minutes to account for temperature regulation. Offset correction values were then calculated using equation (1):

$$O_u = \frac{(N_u^+) + (N_u^-)}{2} \quad (1)$$

where O_u is offset (unitless) along axis u , N_u^+ is raw numeric data indicating position or movement with the gravity vector (unitless) along axis u , and N_u^- is raw numeric data indicating position or movement against the gravity vector (unitless) along axis u . Values of $N_u^{+/-}$ were averaged over 5 data points to better represent fluctuations of the AL101. The calculated offset value (+/-) was then added to the un-normalized data values.

The offset of an accelerometer will also drift due to temperature change. There is an apparent diurnal change in recorded tilt as temperature increases or decreases; this is referred to as temperature coefficient drift. Temperature coefficient drift impacts each axis and accelerometer differently. To account for temperature coefficient drift in calibrating mechanical offset, accelerometers were subjected to artificial temperature fluctuations. Accelerometers were placed in an enclosed cooler with approximately 3 kg of dry ice. A temperature probe was inserted into the cooler and monitored on an external temperature data logger. The system was left in place for ~ 72 hours to allow all dry ice to evaporate, and for the enclosed accelerometers to reacclimate to an ambient room temperature ($\sim 20^{\circ}\text{C}$). The corrected coefficient acceleration values for each axis and accelerometer unit were calculated using the equation (2):

$$A_u = (k_u * ((O_u - N_{ou}) - m_u * (T - t_0))) \quad (2)$$

where A_u is acceleration (g) along axis u , k_u is the proportionality factor (g), O_u is the mechanically offset accelerometer reading (unitless), N_{ou} is the calculated accelerometer offset (unitless), m_u is the proportionality constant (unitless), T is the temperature indicated by the accelerometer ($^{\circ}\text{C}$), and t_0 is the temperature at which the offset calibration was conducted ($^{\circ}\text{C}$).

The proportionality factor was calculated using equation (3):

$$k_u = 1g \frac{(N1_u - N2_u)}{2} \quad (3)$$

Temperature offset was calculated using equation (4):

$$N_{ou} = \frac{(N1_u - N2_u)}{2} \quad (4)$$

The proportionality constant was calculated using equation (5):

$$m_u = \frac{\Delta N_u}{\Delta T} \quad (5)$$

where $N1_u$ and $N2_u$ represent two raw accelerometer readings under two different stable temperature conditions determined in the temperature coefficient experiment. Values $N1_u$ and $N2_u$ were also used to calculate the change in raw data (ΔN_u) under changing temperature conditions (ΔT) to determine the proportionality constant (m_u).

3.2.3 Net Total Tilt Displacement

The monitoring of tree bole tilt changes is mostly concerned with documentation of the y- and z-axes movement as these planes are horizontal (normal) to the gravity vector and are therefore most directly impacted. The AL101 units were mounted vertically, so that the x-axis was parallel to the gravity vector. The projection of the gravity vector onto the y- and z- axes normal to the gravity vector show the magnitude of tree bole displacement or tilt from vertical. Tilt displacement was calculated by using the equation (6):

$$t = \sqrt{y^2 + z^2} \quad (6)$$

where t represents tilt from vertical and y and z represent the axes normal to the gravity vector where tilt is measured. Values of t represent the net total acceleration displacement of the tree bole in response to gravitational forces.

Unfortunately, misalignment of the accelerometer unit in relation to the local gravity vector occurred during the initial installation of field equipment due to the curvature and growing patterns of the tree trunks. As a result, AL101 units were not installed exactly parallel with the gravity vector (i.e., 90°) which presented issues when correlating the net total displacement along the y- and z-axes to wind speed and direction for the white cedar (B2) and red oak (B1). To compensate for this misalignment, a manually selected tilt position was used as the initial tree bole position to compare subsequent values of tilt. Tilt values were subtracted from the manually selected position to determine changes in tilt over time from the initial position. While the most vertical portions of the trunk were chosen for installation to minimize offset with the gravity vector, this procedure needed to be carried out for the white cedar (B2) and the red oak (B1).

Tree physiology and environmental factors were also considered when conducting field work. For example, the stiffness of tree trunks varies with the amount of contained sap as a factor of the modulus of elasticity. Physiological and environmental factors are also sensitive to temperature changes. To avoid a disconnection between temperature and offset values, accelerometers were placed out of direct sunlight and sustained shadows, moderating quick increases and decreases in temperature. However, during periods of canopy loss, the chance of exposure to direct sunlight greatly increased for accelerometers placed on deciduous trees.

Centrifugal forces, defined as the outward force on mass when it is rotated, can affect accelerometer readings, and were also considered during the calibration process. However, these forces were difficult to delineate due to noise in the data and were excluded due to their relatively small influence on tree sway.

3.3 Data Analysis

Un-normalized acceleration data were calibrated to account for mechanical offset and temperature coefficient and converted to units of acceleration (g). The interquartile range (IQR) was determined for each day and axis (x, y, z) for all acceleration data logging units in Excel as a method of filtering noise within the data. Data points between the maximum and minimum limits of the IQR were used for further data analysis. Excel Workbook data were uploaded to RStudio where only data points fulfilling maximum and minimum IQR requirements for all three axes were merged. Datasets for the representative study dates during the months of October, November,

March, and May were created comprising the filtered and merged daily datasets. Continuous data sampling occurred over three-to-five-day intervals for each month of study (October 6-9, 2020, November 16-19, 2020, March 7-10, 2021, May 19-24, 2021). These monthly datasets were then uploaded, and further analyzed in MATLAB.

One hour moving averages were calculated to expose diurnal patterns of movement for each studied tree using the Smoothed Data function in MATLAB. Movement recorded about the y- and z-axes was the primary focus of study as this recorded the swaying movement of the tree bole. Peaks of prominence within the data were determined by conducting a Peak Analysis using the function `findpeaks` in MATLAB. The prominence of a peak measures how much the peak stands out due to its intrinsic height and location in relation to other peaks within a dataset. This shows when the most significant acceleration peaks occur in relation to average movement. Monthly differences in acceleration were analyzed by plotting representative moving-average daily changes over the four different months of recorded data. Wind speed for each month was also included in this analysis to identify the relationship between air movement and tree sway.

Wind data obtained from the RBG Weather Station were analyzed in MATLAB using the Wind Rose function which displays the direction and intensity of wind data and identifies monthly wind direction and intensity trends (Figure 12). Twelve cardinal directions were inputted on the wind rose, and wind speeds in km/h. Wind speeds were divided into six categorical thresholds starting from 0km/h up to > 25km, increasing by units of 5km/h for all monitored days in the months of study. The size of the wedge identified on the wind rose corresponds to the frequency of wind events within that threshold. Percent markers indicate the threshold frequency for each concentric circle. Empty space within the wind rose figure represents no wind events that meet the directional, velocity, and frequency parameters set (Figure 12). To explore the connection between wind speed and tree bole movement, hourly-averaged tilt recorded along the y- and z-axes was plotted against hourly wind speed data in MATLAB for the study dates in each month.

Canopy coverage changes for each of the three trees selected for study were analyzed in conjunction with acceleration and wind data for each month of GLAMA analysis. In this way, the relationship between canopy architecture and the sway movement of trees becomes evident. Special attention was paid to the contrasting responses of deciduous and coniferous species and their differing canopy architectures. To better understand the impacts of canopy architecture on tree sway, canopy openness (%) for each month of study and for each tree of study, accompanied monthly plots of acceleration data.

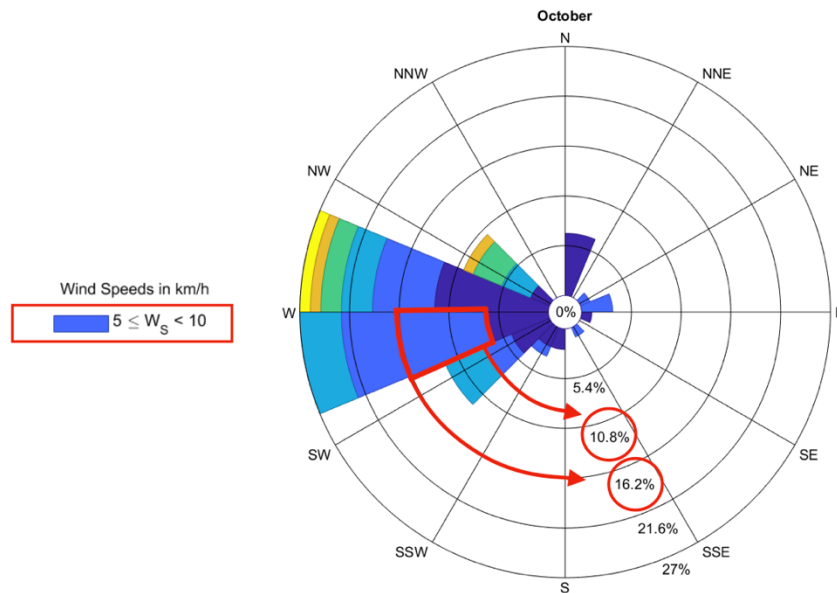


Figure 12: Exemplar wind rose diagram for study dates in October 2020. The red wedge outlined on the wind rose diagram indicates the frequency of wind events reaching speeds (W_s) between 5-10km/h for the study dates in October.

3.3.1 Statistical Analysis

Correlations between variables such as wind speed (km/h) and direction ($^{\circ}$), tree sway (acceleration), and canopy coverage were determined using RStudio statistical software. Data were considered to be normally distributed after performing a box plot assessment in which $> 95\%$ of data fell within the fences. A Shapiro-Wilkes test of normality to assess acceleration data could

not be performed due to entry volume limitations (max. 5000 entries). To determine the strength of the correlation between tree sway and modified canopy coverage and month for each accelerometer unit in the dataset, a one-way Analysis of Variance (ANOVA) test was performed. A Tukey post hoc analysis was then completed for variables displaying a significant difference ($p < 0.05$). Homoscedasticity was assumed when performing the Tukey post hoc assessment. To determine the general correlation between wind and acceleration dataset variables, and the changes within the study period, Pearson’s r value for wind speed and acceleration, wind direction and acceleration, and time and acceleration along the y - and z -axes was calculated for each month of the study.

Table 3: Summary statistics identifying correlations between wind speed and acceleration along the y -axis for each month of study for each tree species examined in this research. Correlations were determined by performing a Pearson product-moment correlation coefficient. P -values < 0.05 are considered statistically significant results.

Month	Pearson r correlation values (p -value)		
	Red oak (B1)	White cedar (B2)	Sugar maple (R1)
October	2.772e-10	0.8978	0.4177
November	6.687e-05	0.007109	0.001472
March	0.1969	0.004922	0.1246
May	0.9349	0.001103	1.532e-07

4. Results

4.1 Vegetation Catalogue

Distinct terrestrial vegetation communities along the escarpment in Hamilton are coupled with physical aspects of the escarpment gradient. The transition from mature forest plateaus to exposed lichen-covered bedrock faces and shrub dominated talus slopes, exemplifies how the physical environment regulates the type and productivity of vegetation (Larson *et al.*, 1989). A broad physical and biological description of escarpment vegetation in Hamilton was catalogued at the Chedoke Radial Trail and Rockcliffe Trail locations. The escarpment gradient was subdivided into three major sections (Figure 13); upper and intermediate escarpment plateaus and ledges, bedrock face, and sloping talus.

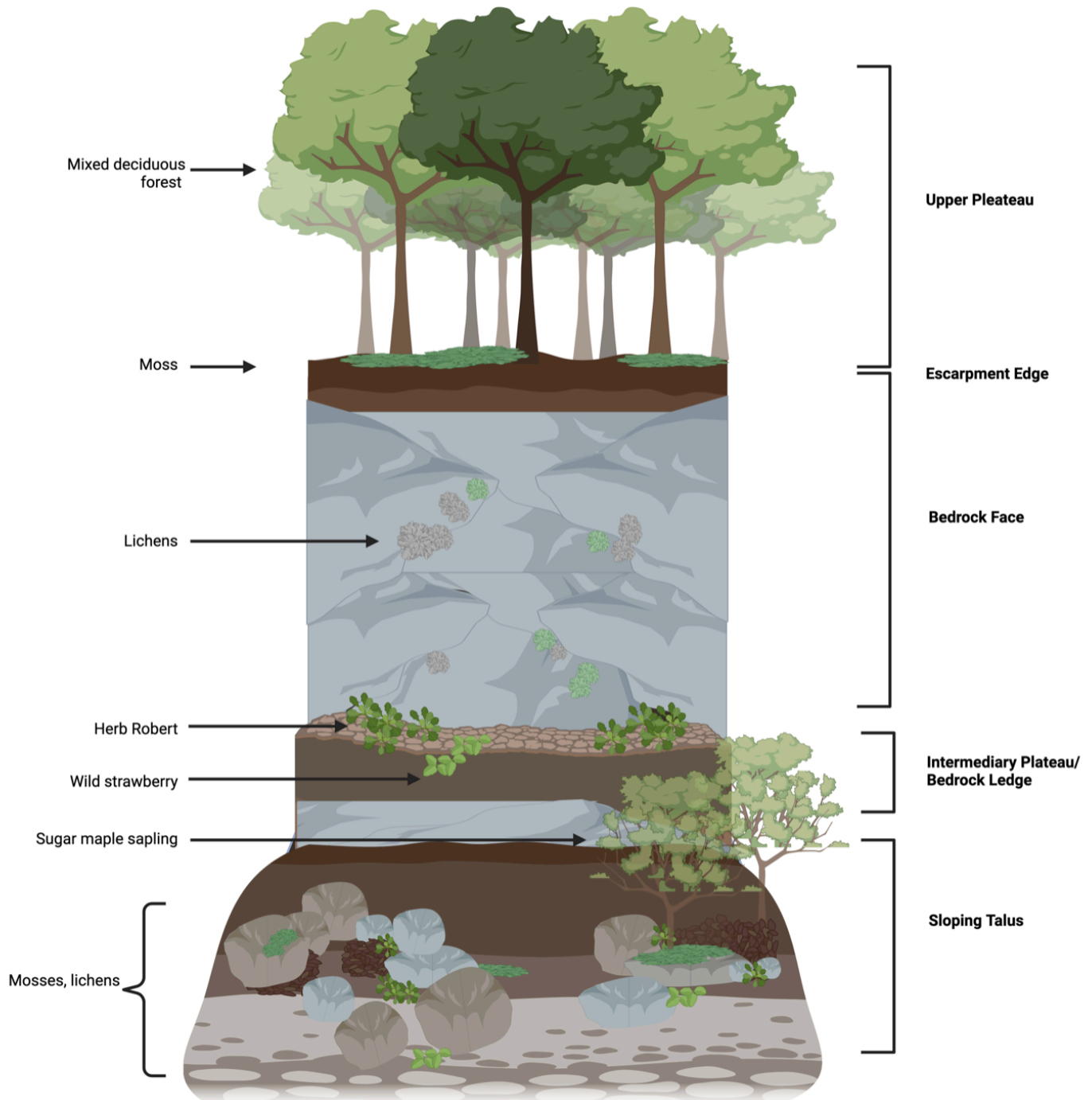


Figure 13: A simplified vertical transect of escarpment vegetation in Hamilton (not to scale). Patterns of plant growth and development can be related to the position on the escarpment: upper plateau, bedrock face, intermediary plateau (ledges), and sloping talus (Created using BioRender.com).

4.1.1 Upper and Intermediate Plateau and Ledges

On the upper plateau, woody vegetation such as trees and tall shrubs were often in the same abundance as low-lying shrubs and herbaceous plants (Figure 13). Large trees (DBH >15 cm) such as sugar maple (*Acer saccharum*) and white birch (*Betula papyrifera*), were observed almost exclusively on the upper plateau at the top of the escarpment (Table 2). Intermediary plateaus and bedrock ledges along the Radial Trail also provided conditions for large tree growth; however, diameter at breast height (DBH) of these trees was often less than trees at the top of the escarpment (>5cm DBH <15cm; Figure 13). Intermediary plateaus are defined in this research as any level terrain beneath the upper plateau along the escarpment slope that can support large tree growth.

There was a clear shift in species abundance as the escarpment edge was approached, as soil depth decreased, and exposure to incoming solar radiation increased. The escarpment edge is defined in this research as the position on the upper escarpment slope where the horizontal plateau transitions to the vertical bedrock face. At the escarpment edge, and across the bedrock face, soil depths were observed to be near zero except within small vugs, and along bedrock ledges that accumulate transient soil from the overlying plateau. The plant community found here was composed of stress-tolerant species such as moss (*Brachythecium salesbrosum*) and herb Robert (*Geranium robertianum*), species able to adapt to high degrees of exposure and rapid fluctuations in environmental conditions (Table 2).

4.1.2 Bedrock Face

On the bedrock face, there are few large trees and tall shrubs, with the exception of white cedar (*Thuja occidentalis*); herbaceous and non-vascular plants such as moss (*Brachythecium salesbrosum*) and lichen dominate (Figure 13 and Table 2). White cedar species were only present along the cliff edge or on the cliff face at the Rockcliffe Trail study site and were not present at the study site along the Radial Trail. In fact, there was no evidence of coniferous tree growth at any of the Radial Trail transects. The forest community here was dominated by broadleaved deciduous trees such as sugar maple (*Acer saccharum*) and red oak (*Quercus rubra*). Lichens were also noted on the cliff face and their abundance in this zone exceeded that of any other plant group (Larson *et al.*, 1989; Table 2).

Table 2: List of species and corresponding position along the topographic gradient of the escarpment in Hamilton.

Section of gradient	Plateaus	Cliff Ledges & Vugs	Bedrock Face	Sloping Talus
Plant Groups				
Non-Vascular Plants & Other		Moss (<i>Brachythecium salesbrosom</i> , <i>Anomodon minor</i>)	Moss (<i>Brachythecium salesbrosom</i> , <i>Anomodon minor</i>) Lichens.	
Groundcover & Shrubs	Honeysuckle (<i>Diervilla lonicera</i>) Sumac (<i>Rhus typhina</i>) Red raspberry (<i>Rubus idaeus</i>) Poison ivy (<i>Toxicodendron radicans</i>)	Goldenrod (<i>Solidago canadensis</i>) Honeysuckle (<i>Diervilla lonicera</i>) Sumac (<i>Rhus typhina</i>) Herb Robert (<i>Geranium robertianum</i>) Wild strawberry (<i>Fragaria virginiana</i>)		Goldenrod (<i>Solidago canadensis</i>) Honeysuckle (<i>Diervilla lonicera</i>) Sumac (<i>Rhus typhina</i>) Red raspberry (<i>Rubus idaeus</i>)
Saplings		Mountain maple (<i>Acer spicatum</i>) White cedar (<i>Thuja occidentalis</i>)		Mountain maple (<i>Acer spicatum</i>) White ash (<i>Fraxinus americana</i>)
Open Canopy (>10% - <40% density)	Sugar maple (<i>Acer saccharum</i>) White ash (<i>Fraxinus americana</i>)		White cedar (<i>Thuja occidentalis</i>)	
Closed Canopy (>40% density)	Sugar maple (<i>Acer saccharum</i>) White birch (<i>Betula papyrifera</i>) White cedar (<i>Thuja occidentalis</i>) Red oak (<i>Quercus rubra</i>)			

4.1.3 Sloping Talus

Escarpment talus slopes are formed by the accumulation of clastic debris below the bedrock face and plateau (Figure 13). Increased radiation and moderate soil depths on the talus slopes are intuited to foster high levels of primary productivity at this location on the escarpment face. However, all species in this location are exposed to increased physical abrasion and disturbance from falling bedrock (Larson, *et al.*, 1989). Therefore, vegetation on talus slopes was often relatively small in stature and showed typical disturbance-based characteristics such as the growth of new shoots from the root base, or through underground rhizomes (Bernard, 1990). Plant cover on recently mobile talus was found to be particularly sparse and where present, consisted of small,

vascular species such as sedges (*Carex*), goldenrod (*Solidago canadensis*) and wild strawberry (*Fragaria virginiana*). On talus covered by old, larger blocks of failed bedrock, vegetation cover was greater due to the increased protection offered in the lee of blocks (Perez, 2012) (Figure 13 and Table 2).

4.2 Wind-Induced Sway

Trees have characteristic swaying patterns impacted by their size, canopy and trunk shape, and material properties such as elasticity (Jackson *et al.*, 2021). To quantify the influence of tree sway and forces on escarpment bedrock, triaxial accelerometers were mounted onto tree boles to determine (1) diurnal and monthly patterns of movement in relation to wind intensity, frequency, and direction, and (2) how seasonal canopy changes impact tree motion characteristics. The data obtained from the three accelerometer units were tested for correlations with meteorological data by using one-way ANOVA tests and Pearson's test of correlation in which p -values of <0.05 are considered statistically significant and R^2 values of <0.5 indicate a strong correlation.

Combined acceleration values along the y - and z -axes, obtained from the AL101 units, are indicative of tree bole tilt. These values show the angular difference between the gravity vector and the projected gravitational forces onto the axes normal to gravity (i.e., y - and z -axes) that result in tilt movements. Tilt can occur in both the positive ($+y/+z$) and negative ($-y/-z$) directions (Figure 14 and Figures 15-18). The AL101 accelerometer utilizes a right-handed coordinate system as a frame of reference and numeric sign does not indicate the presence or absence of movement in this context, but rather indicates the direction of tilt along the planes of the y - and z -axes (Figure 14). However, using the square-root of the sum of squares (Equation 6 above) to depict the net total acceleration displacement of the tree bole, all values of tilt are positive integers. Therefore, a greater positive value indicates an increase of tilt from vertical along the y - and z -axes, and a lesser positive value indicates a return to a vertical, resting position (Figure 14). Calculated values are representative of a change in acceleration magnitude or net total acceleration displacement along the y - and z -axes which implies a tilt away from the vertical position (Wagner, personal communication, 2022). The magnitude of tilt along the y - and z -axes from resting, recorded by fluctuations in acceleration by the AL101 units, is indicative of tree bole sway. Tree sway may be linked to wind-driven root movement and used as a proxy for estimating processes contributing to

bedrock erosion, as suggested in previous research (Marshall, 2018). Results of this previous research determined that forces generated through the sway movement of trees in response to wind was an important mechanism contributing to forces at the root-bedrock interface, with potential to exacerbate bedrock weathering over time (Marshall, 2018; Jimerson 2020).

4.2.1 Acceleration Trends

Net acceleration displacement and patterns of movement between tree species were identified for study days in each month of study (October, November, March, and May; Figures 15-18). These values depict the magnitude of tilt from vertical that occurred along the tree bole of each tree studied utilizing a gravitational frame of reference. A higher tilt value (g) indicates greater tilt from vertical and a decline in tilt value indicates movement back through vertical. Tilt oscillations were significantly different for each tree species examined in this study; however, all species recorded the greatest tilt during average daylight hours and least during average nighttime hours (Figures 15-18).

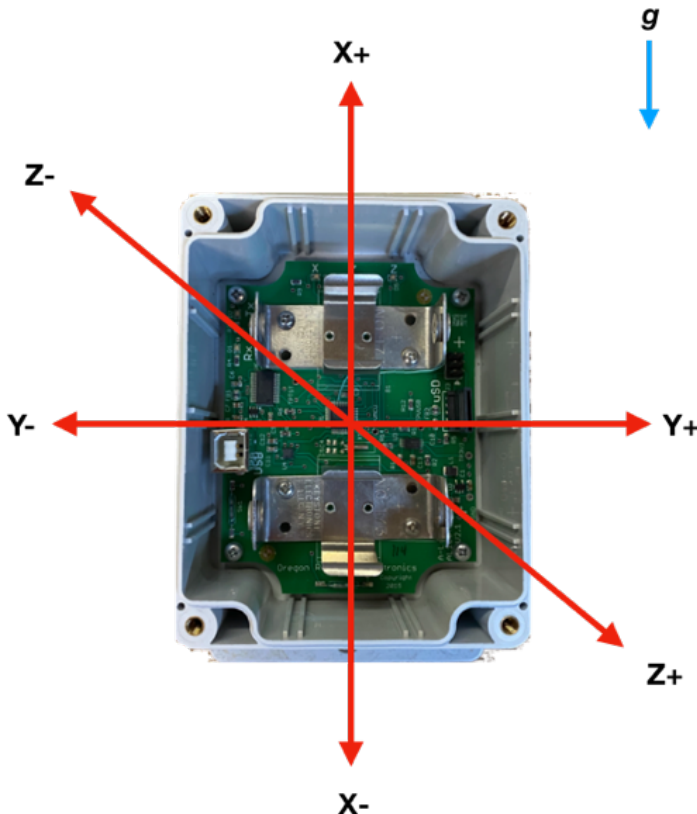


Figure 14: A right-hand coordinate system superimposed on the AL101 triaxial accelerometer. Each of the three axes (x, y, z) are identified including both positive and negative planes. The x-axis is in alignment with the gravity vector, indicated by the blue arrow, in the vertical position.

Tilt values recorded along the y- and z-axes by the AL101 triaxial accelerometers were also plotted against wind speed data for study days in each month of study to discern any meaningful relationship between tree sway and air movement (dashed grey line; Figures 15-18). Any contrast in the response of deciduous and coniferous species will help determine if tree species and canopy changes have a significant impact on the relationship between wind excitation and tree bole tilt. This information can inform which tree species may be most at risk of causing root movement in bedrock joints and in which season.

4.2.1.1 Diurnal Movement

Tree bole tilt along the y- and z-axes recorded by all three AL101 units shows a strong correlation with time of day for all study days ($p = < 0.05$; Figures 15-18). This correlation was determined by contrasting acceleration during average daylight hours (06:00-18:00) and acceleration during average nighttime hours (19:00-05:00) for all units and days of study (Figures 15-18). The results indicate that there is a significant difference between tree bole tilt during the day and tree bole tilt at night. Tree bole tilt was greatest (recorded by increased acceleration values) between the hours of 10:00–14:00 in October and November, and between 12:00-18:00 in March and May (Figures 15-18). This result may be impacted by diurnal patterns of air movement on the escarpment caused by temperature differences between day and night (Chellali *et al.*, 2013). The intrinsic relationship between wind speed and insolation is therefore suggested to impact tree sway forces at these times (Figures 15-18).

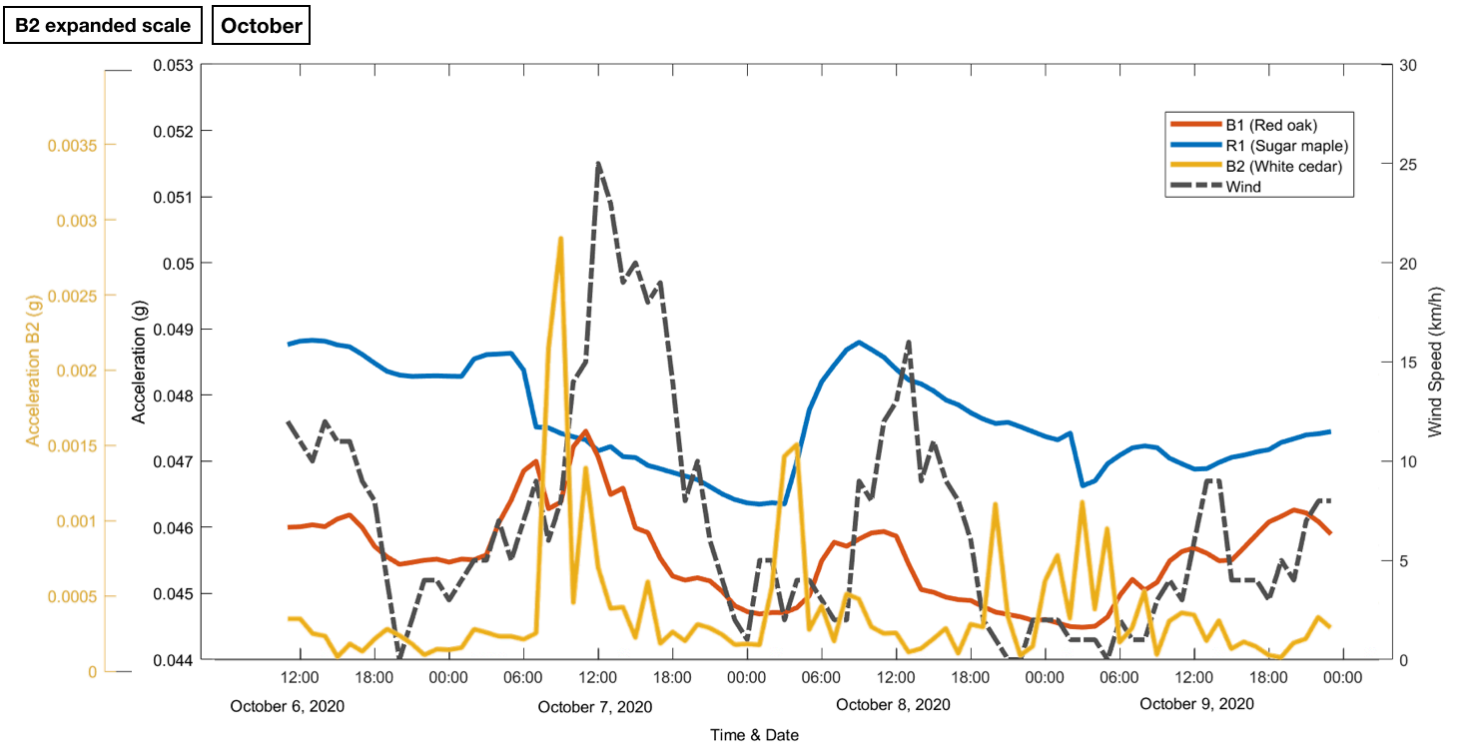


Figure 15: The relationship between acceleration along the y- and z-axes and wind speed for the studied days in the month of October, 2020. Tree bole tilt is depicted by acceleration(g) for unit B1(red), unit B2 (yellow), and unit R1(blue). Wind speed (km/h) is indicated by the dashed grey line. Increased tilt along the y- and z-axes are indicated by increasing values of acceleration(g). Unit B2 (yellow) is plot on a secondary y-axis to better show diurnal variation of tilt. Due to discrepancies in the angle of accelerometer placement, a correction factor has been added to original acceleration data for the white cedar (B2; yellow; see page 43 for further explanation of this correction).

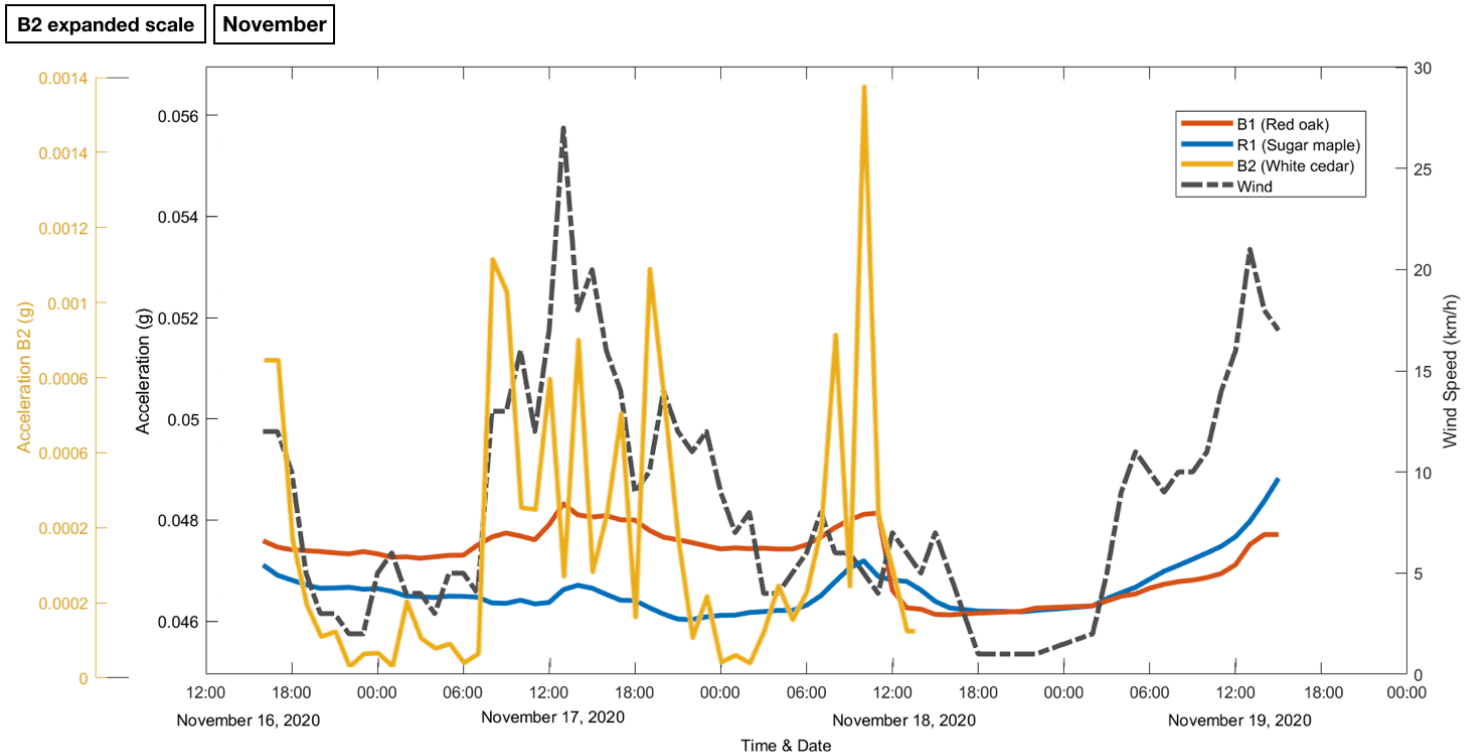


Figure 16: The relationship between acceleration along the y- and z-axes and wind speed for the studied days in the month of November. Tree bole tilt is depicted by acceleration(g) for unit B1(red), unit B2 (yellow), and unit R1(blue). Wind speed (km/h) is indicated by the dashed grey line. Increased tilt along the y- and z-axes are indicated by increasing values of acceleration(g). Unit B2 (yellow) covers a shorter period of time due to an issue with battery-life. Unit B2 (yellow) covers a shorter period of time due to an issue of battery-life. Unit B2 (yellow) is plot on a secondary y-axis to better show diurnal variation of tilt. Due to discrepancies in the angle of accelerometer placement, a correction factor has been added to original acceleration data for the white cedar (B2; yellow; see page 43 for further explanation of this correction).

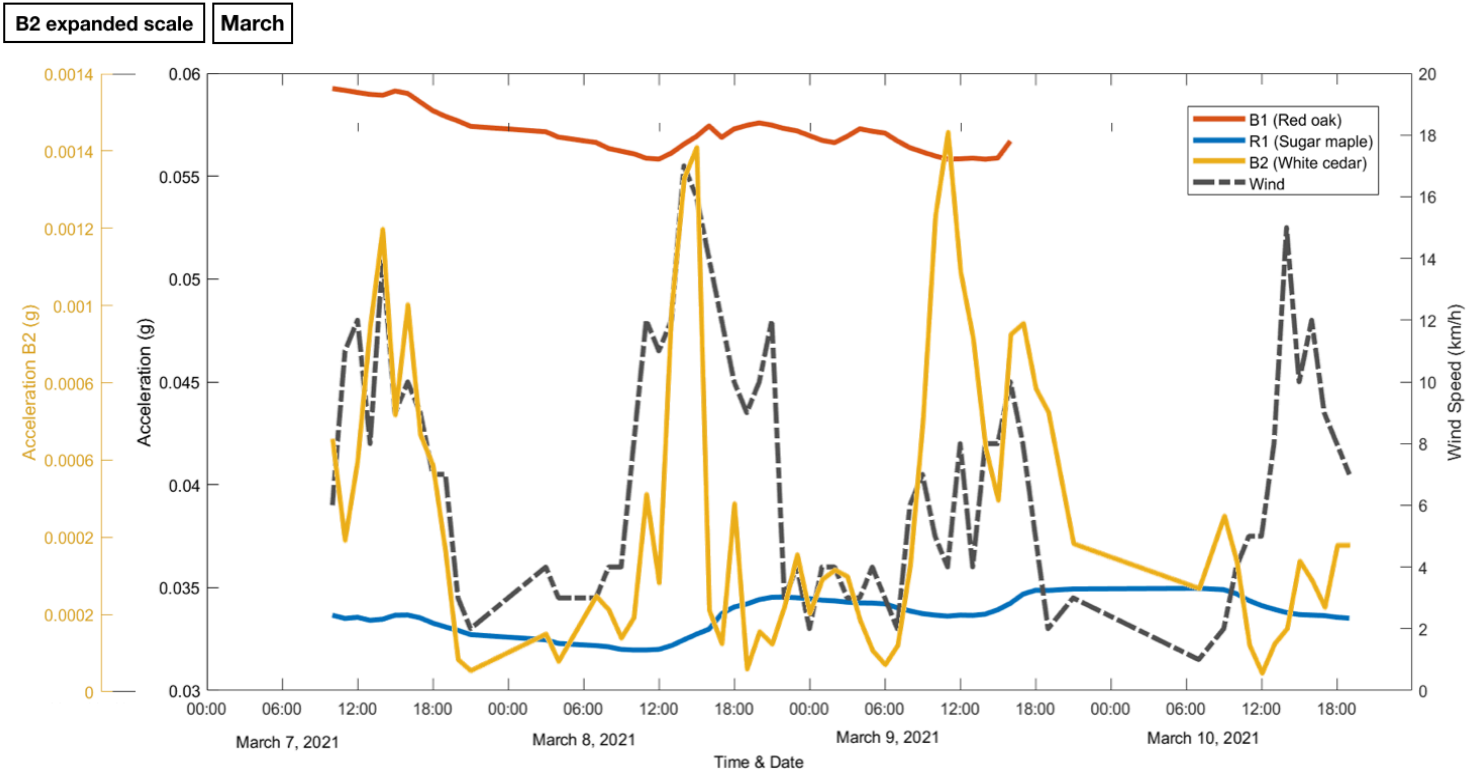


Figure 17: The relationship between acceleration along the y- and z-axes and wind speed for the studied days in the month of March. Tree bole tilt is depicted by acceleration(g) for unit B1(red), unit B2 (yellow), and unit R1(blue). Wind speed (km/h) is indicated by the dashed grey line. Increased tilt along the y- and z-axes are indicated by increasing values of acceleration(g). Unit B1 (red) covers a shorter period of time due to an issue of battery-life. Unit B2 (yellow) is plot on a secondary y-axis to better show diurnal variation of tilt. Due to discrepancies in the angle of accelerometer placement, a correction factor has been added to original acceleration data for the white cedar (B2; yellow; see page 43 for further explanation of this correction).

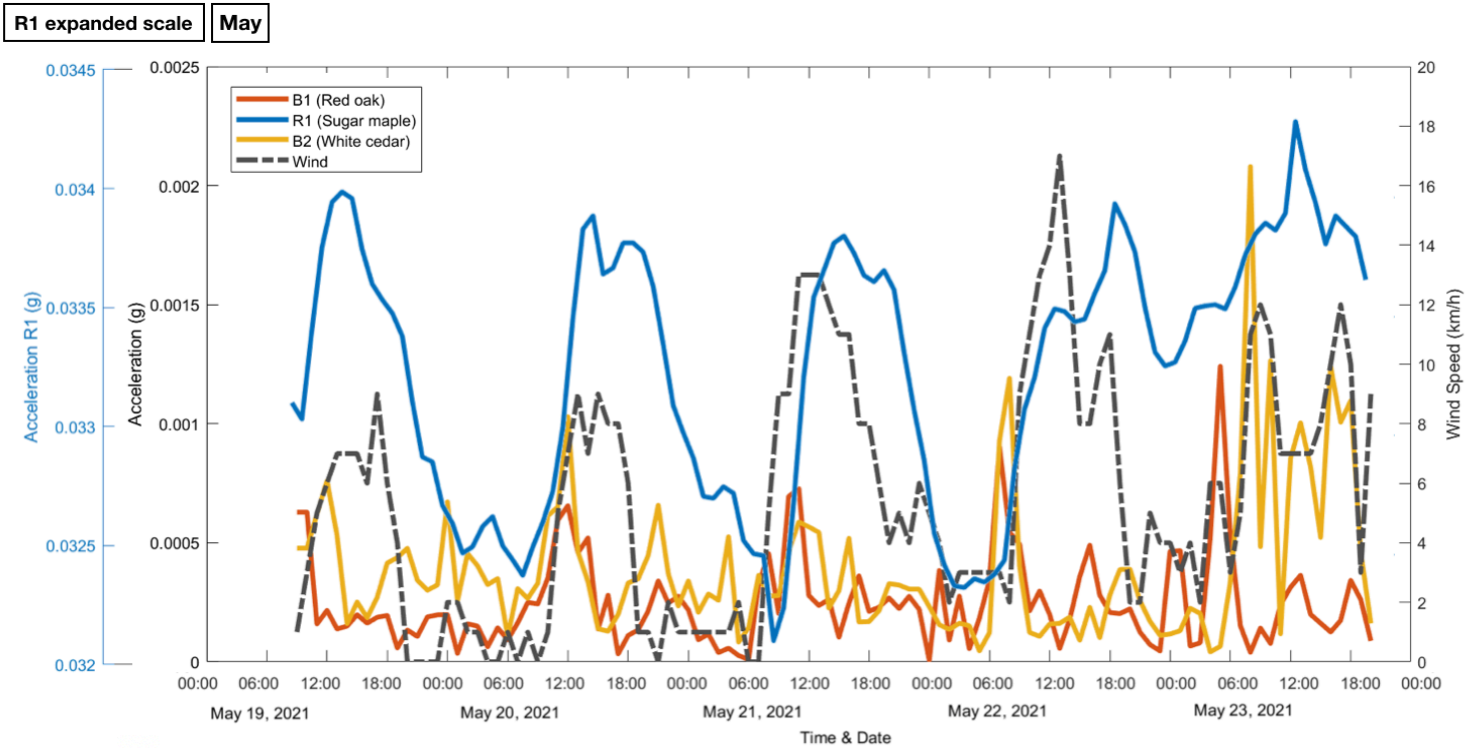


Figure 18: The relationship between acceleration along the y- and z-axes and wind speed for the studied days in the month of May. Tree bole tilt is depicted by acceleration(g) for unit B1(red), unit B2 (yellow), and unit R1(blue). Wind speed (km/h) is indicated by the dashed grey line. Increased tilt along the y- and z-axes are indicated by increasing values of acceleration(g). Unit R1 (red) was plot on a secondary y-axis to better show diurnal variation of tilt. Due to discrepancies in the angle of accelerometer placement, a correction factor has been added to original acceleration data for the white cedar (B2; yellow) and the red oak (B1; red; see page 43 for further explanation of this correction).

4.2.1.2 Data Correction

Tree physiological properties, particularly related to the growth angle of the tree bole, likely have a strong impact on recorded tilt results in this research. The AL101 senses a resting, vertical posture of 90 degrees and measures tilt away from vertical along the horizontal planes (y- and z-axes). Movement through the AL101 vertical position is recorded as a tilt back to resting or a decrease in acceleration. Unfortunately, the angle of accelerometer placement on the white cedar (B2) was not at 90 degrees and any tilt through vertical was recorded as movement back to resting, but in reality coincided with tilt away from resting. The accelerometer records from B2 incorrectly identified declines in tilt during increased wind speeds, and cumulative increases in tilt from successive wind events. To mitigate these discrepancies, the manufacturer of the accelerometer units recommended calculating the magnitude of deflection from the growth position of the white cedar (B2) to correct these data (Wagner, per. comm., 2022; Figures 15-18). Hence, a secondary axis is utilized to depict the corrected tilt values of the white cedar (B2) on Figures 15-17; the original data for the white cedar (B2) are plotted together with data from the sugar maple (R1) and red oak (B1) in Appendix A (Figures A1-A4).

A similar discrepancy was noted in the accelerometer data collected for the red oak (B1) in May, which also recorded successive increases of bole tilt along the y- and z-axes during each wind event, with no recoil back to vertical. It remains unclear as to why discrepancies within the data only occurred in May records for the red oak (B1) but may have reflected changes to the tree growth position. Hence, a similar correction factor was applied to the red oak (B1) values collected in May, subtracting the recorded values from the manually selected vertical position to better represent the relationship between tilt and wind speed (Figure 18). A secondary axis is utilized to depict tilt values of the sugar maple (R1) for the study dates in May as it was the only unit that did not require further data correction and thereby possesses a different acceleration value range (Figure 18). The original data for the red oak (B1) on the study dates in May are plotted together with data from the sugar maple (R1) and white cedar (B2) in Appendix A (Figure A4).

4.2.1.3 Seasonal Movement

During March, the sugar maple (R1), red oak (B1), and white cedar (B2) recorded distinctly different patterns of acceleration with movement of the white cedar (B2) being most closely related to increased wind speed (Figure 17). It is possible that the absence of canopy cover on the deciduous trees may have reduced their response to increased wind speed at this time. The transition from March, with the lowest canopy coverage, to May with the greatest canopy coverage may have impacted the dissipation of wind energy and the resonance forces acting on the tree boles (Quine & Gardiner, 2007; Gardiner *et al.*, 1997).

Overall, the disparity between the way in which the deciduous trees, red oak (B1) and sugar maple (R1), and the coniferous tree, white cedar (B2), reacted to wind events suggests that a strong relationship exists between tree species and the way in which wind energy is dissipated. Recorded movements along the y- and z-axes were significantly different ($p = < 0.0001$) for the conifer (white cedar, B2) and deciduous trees (red oak (B1) and sugar maple (R1)) monitored in this study; in addition, there were meaningful differences ($p = < 0.0001$) in recorded acceleration values between the red oak (B1) and the sugar maple (R1). These results support the idea that wind loading, and resulting tree sway motions, are different for coniferous and deciduous tree species (Quine & Gardiner, 2007), and between different broadleaved species. However, these are preliminary findings from only three monitored trees and the relationship between tree species and wind loading requires further investigation.

4.3 Environmental Variables and Acceleration

4.3.1 Wind Speed

On the days in the months of October, November, March, and May used in this study, the highest wind speeds (>25 km/h) recorded at the Royal Botanical Gardens Weather Station occurred during October and November, and the lowest wind speeds (<15 km/h) occurred during March and May (Figure 19). The highest wind speeds for each study day typically occurred between the hours of 10:00 - 14:00.

Correlations between wind speed and acceleration along the y- and z-axes were different for each month and varied for all trees in this study (red oak (B1), sugar maple (R1), and white cedar (B2); Figures 15-18). Tilt along the y- and z-axes of the red oak (B1) was most strongly correlated to wind speed during October and November (Table 3). Similarly, the sugar maple (R1) exhibited a correlation between tilt along the y- and z-axes and wind speed during November, but also exhibited a strong correlation during March (Table 3). The white cedar (B2) exhibited a strong correlation to wind speed in each month of the study except for October (Table 3). These results suggest that wind speed does have an important impact on tree bole tilt from vertical for trees in this study. However, the variability of recorded tree tilt in response to changing wind speed may also be impacted by species physiological factors such as DBH, tree bole plasticity, and canopy architecture, in addition to factors such as growth position within the forest stand and the mounted position of the accelerometers. These factors all impact the dissipation of wind forces, canopy drag and collision force, and the resonance forces on the tree bole (Quine & Gardiner, 2007; Gardiner *et al.*, 1997). These biotic and abiotic components may contribute more significantly to tree sway motions during those months presenting a weak correlation. In addition, wind flow in and above forested areas is highly turbulent, and wind speed is not a standalone component of wind loading on trees (Moore *et al.*, 2018). Wind gusts formed by the rapid increase in horizontal wind speed and the downward movement through the canopy exert forces that are estimated to be ten times larger than those of mean wind speed and may have greater control of tree sway movement (Moore *et al.*, 2018; Gardiner *et al.*, 1997). An additional, and very likely source of error in this study, is due to the geographic distance between the RBG weather station and research sites along the escarpment; both wind speed and direction at the research sites could differ significantly to those recorded by the weather station. Hence, a firm conclusion concerning the relationship between wind speed, direction and tree bole movement cannot be made from this study.

Table 3: Summary statistics identifying correlations between wind speed and acceleration along the y-axis for each month of study for each tree species examined in this research. Correlations were determined by performing a Pearson product-moment correlation coefficient. P-values < 0.05 are considered statistically significant results.

Month	Pearson r correlation values (<i>p</i> -value)		
	Red oak (B1)	White cedar (B2)	Sugar maple (R1)
October	2.772e-10	0.8978	0.4177
November	6.687e-05	0.007109	0.001472
March	0.1969	0.004922	0.1246
May	0.9349	0.001103	1.532e-07

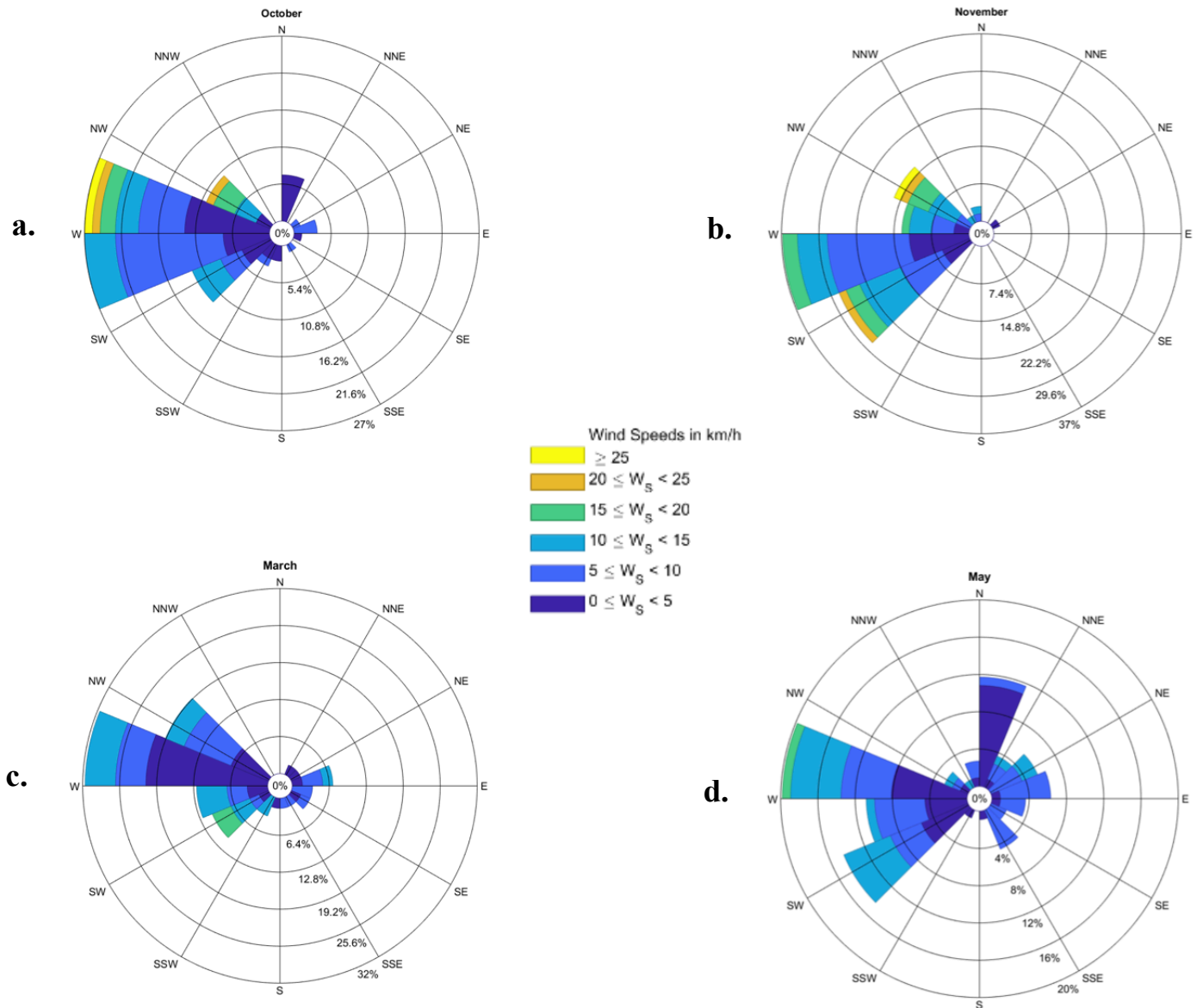


Figure 19: Wind rose diagrams for study dates in (a) October, (b) November, (c) March, and (d) May. Wind direction is displayed by cardinal direction on the perimeter of the diagram, and wind speed (km/h) is represented by colour. Wind speeds were subdivided into categories, starting from 0 km/h and increasing at intervals of 5 km/h. Each concentric circle within the rose corresponds to the frequency (%) of wind events from a certain direction and speed category. Frequency is indicated by a percentage and vary for each month of study.

4.3.2 Wind Direction

On the days in the months of October, March, and May used in this study, the dominant wind direction was west-northwest; in November wind direction was dominantly west-southwest (Figure 19). The directionality of wind was determined to be correlated to tilt along the y-and z-axes for the monitored deciduous tree species, red oak (B1), and sugar maple (R1). Tree tilt and wind direction were correlated for all months of study for the red oak (B1) and all months except for October for the sugar maple (R1), while directionality of wind had no statistical influence on bole tilt for the conifer in this study (white cedar (B2)) (Table 4). The strength of correlation between tree sway tilt along the y-and z-axes and wind direction is likely impacted by the cardinal direction in which each tree in this study faces (Table 1) as well as the orientation of the escarpment. The recorded tilt along the y-and z-axes for the sugar maple (R1) and red oak (B1) is closely aligned with wind direction, which may strongly impact the amplitude of tilt recorded. The exposed growth position of the white cedar (B2), which lies on the edge of the escarpment, may make it more susceptible to tilt during periods of high wind speed, rather than from winds from a particular direction.

Table 4: Summary statistics identifying correlations between wind direction and acceleration along the y-axis for each month of study and each tree species examined in this research. Correlations were determined by performing a Pearson product-moment correlation coefficient. P-values < 0.05 are considered statistically significant results.

Month	Pearson r correlation values (<i>p</i> -value)		
	Red oak (B1)	White cedar (B2)	Sugar maple (R1)
October	0.002508	0.8978	0.1716
November	0.0002931	0.7723	0.002322
March	0.003769	0.1016	0.01505
May	0.04028	0.9621	0.03207

4.3.3 Canopy Cover

Modified canopy cover (CaCo) recorded using GLAMA was highest during May and October, and greatest at site R1 with a maximum CaCo value of 83% (Figure 20). There was no significant difference ($p = 0.559$) between seasonal canopy cover for any of the three trees monitored in this research project. However, leaves and boughs of neighboring trees were often included in the GLAMA assessments of CaCo due to the mixed deciduous canopy surrounding each monitored tree (Figures 21-23). More precise evaluation of the impact of canopy cover on tree sway could be determined by documenting seasonal canopy architecture of standalone trees. The CaCo data collected in this study show meaningful changes in CaCo ($p = 1.28e-13$) at each study site during seasonal transitions, such as fall (October) to winter (November). Due to the coupled nature of wind loading and canopy architecture, seasonal transitions marked by the loss or gain of leaves, particularly in deciduous species, may signify periods of increased drag forces and tree sway. Loss of leaves tends to increase wind penetration into the canopy and increase loading on tree boles (Quine & Gardiner, 2007).

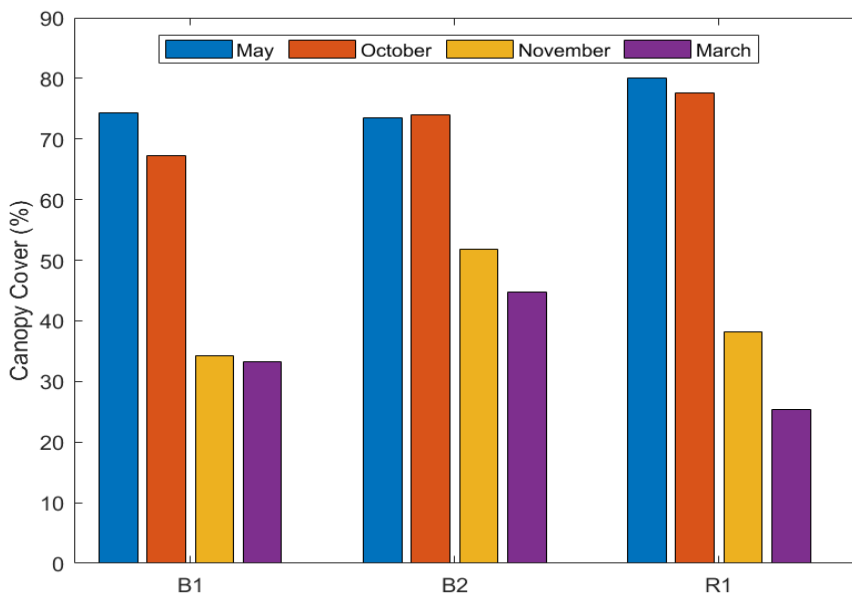


Figure 20: Bar plot depicting changes in modified canopy cover (%) calculated using GLAMA. Canopy cover measurements were taken for each of the four months of study; May (blue), October (orange), November (yellow), and March (purple). B1 (red oak), B2 (white cedar), and R1 (sugar maple) study sites (Figures 21-23).

Chronic wind loading increases the likelihood of acute tree bole failure and can intensify biomechanical weathering processes when tree roots are in contact with bedrock (Pawlik *et al.*, 2016). The pattern of tree bole tilt documented in this study fluctuates between each month of study and for each tree species as the forest canopy cycles through periods of leaf loss and leaf gain (Figures 15-18 and Figure 20). Although it is likely that an inverse relationship exists between CaCo and acceleration along the y- and z-axes for the trees monitored in this study, this cannot be confirmed due to the absence of CaCo data specific to each monitored tree.

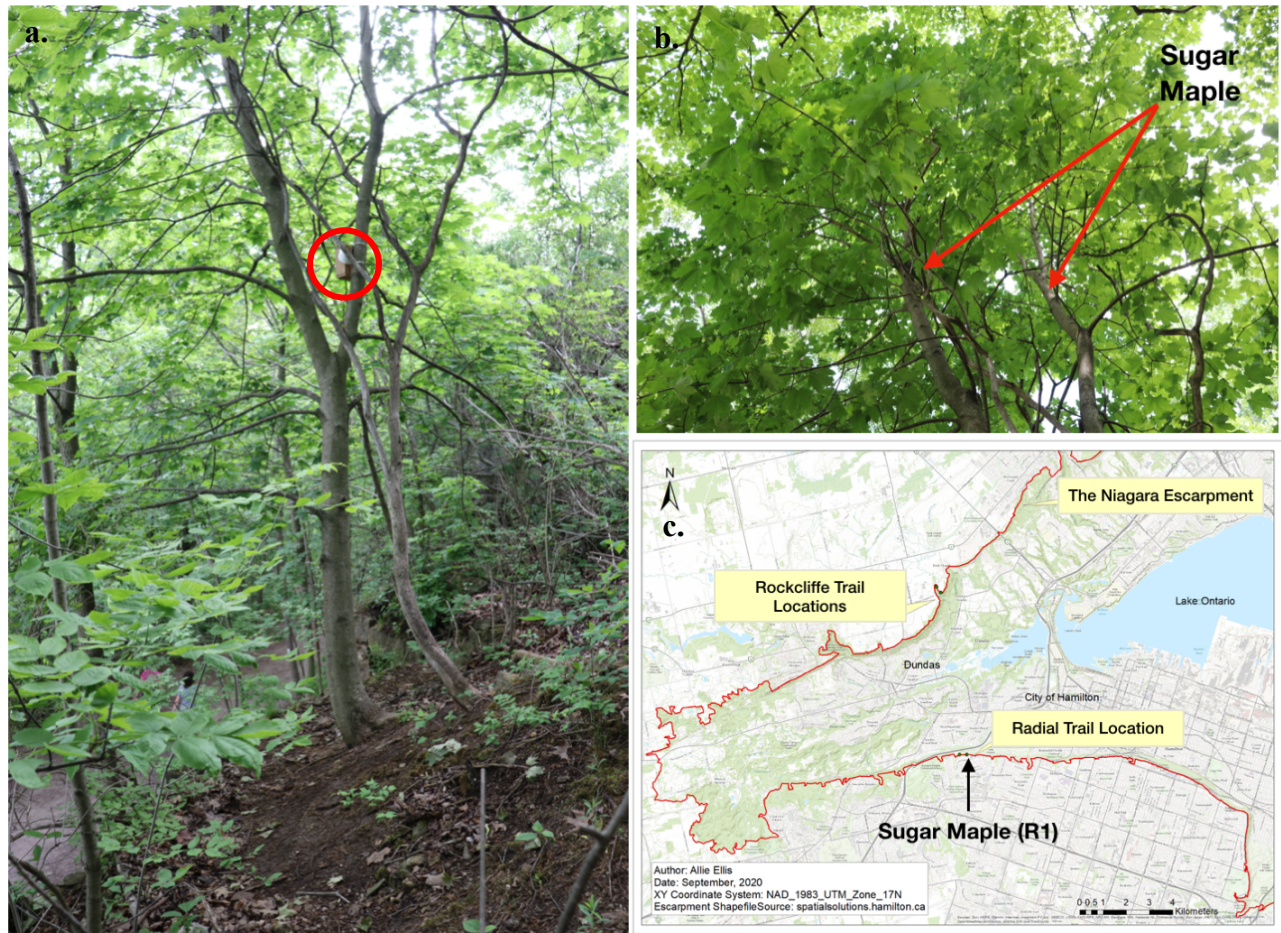


Figure 21: (a) mounted AL101 on the sugar maple (R1) and surrounding forest structure located along the Chedoke Radial Trail, (b) canopy view of the sugar maple (R1) and overlying canopy architecture, (c) map of fieldwork locations along the Niagara Escarpment and highlighting the location of the sugar maple (R1).

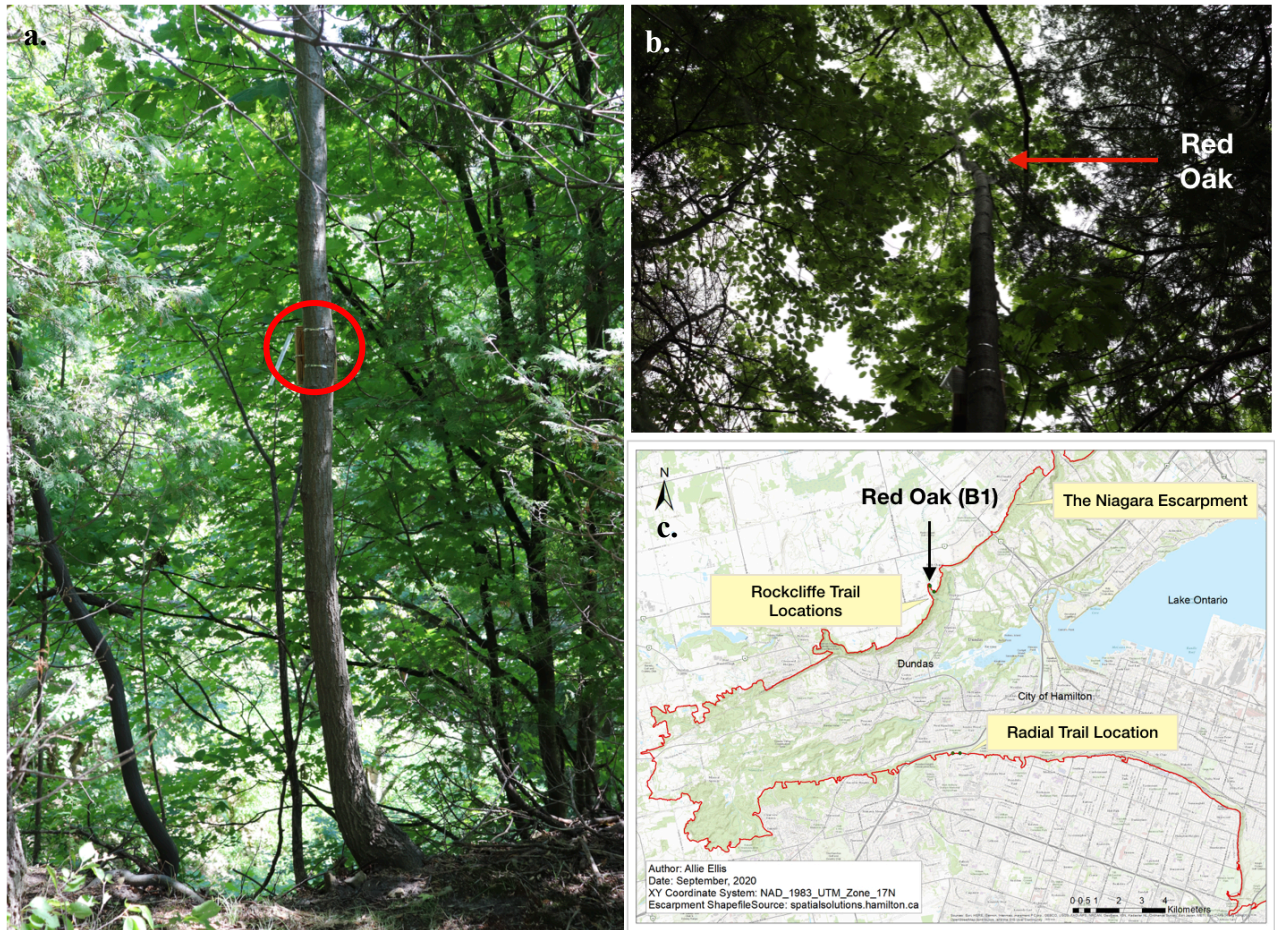


Figure 22: (a) mounted AL101 on the red oak (B1) and surrounding forest structure located along the Rockcliffe trail, (b) canopy view of the red oak (B1) and overlying canopy architecture, (c) map of fieldwork locations along the Niagara Escarpment and highlighting the location of the red oak (B1).

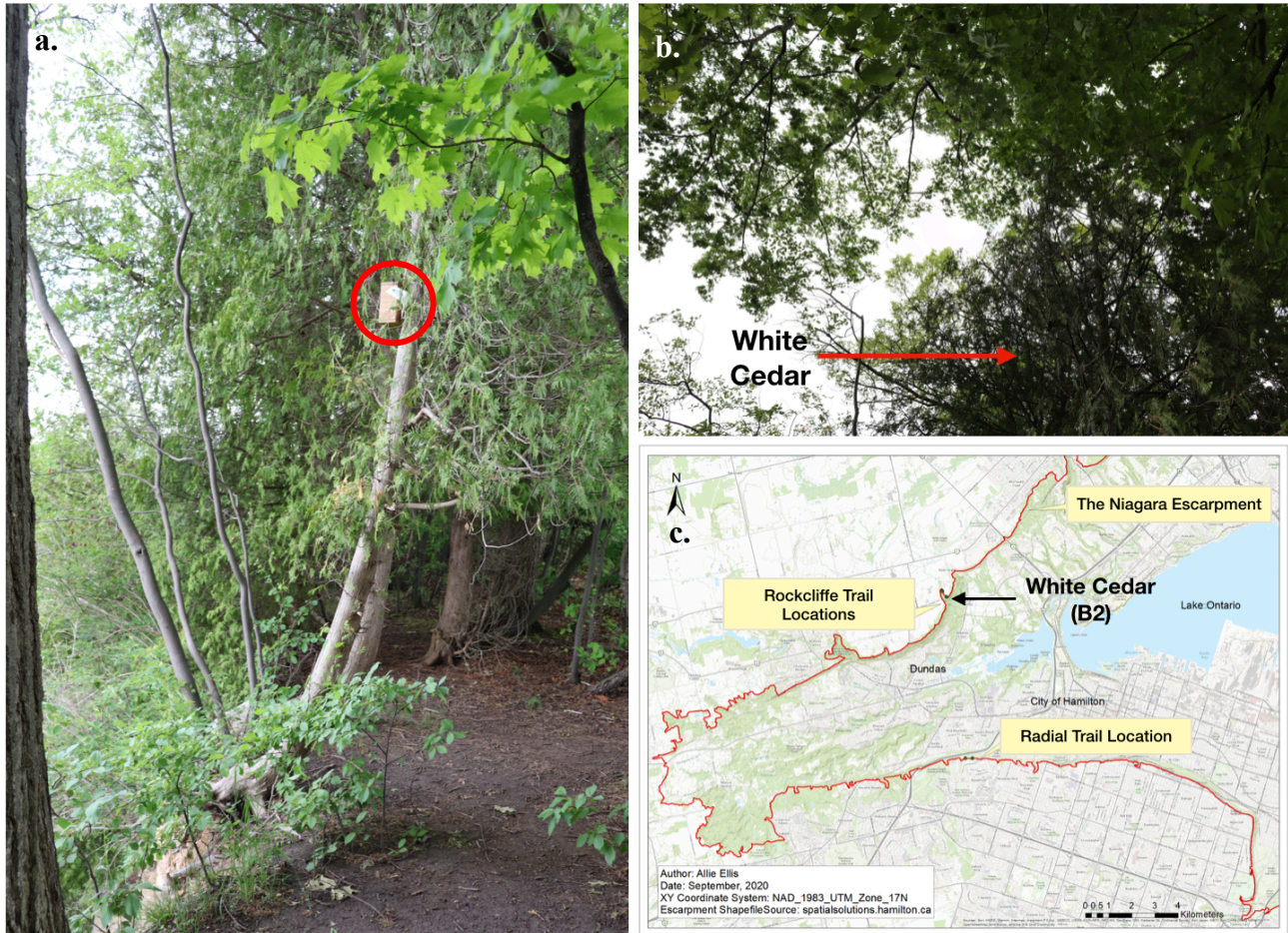


Figure 23: (a) mounted AL101 on the white cedar (B2) and surrounding forest structure located along the Rockcliffe trail, (b) canopy view of the white cedar (B2) and overlying canopy architecture, (c) map of fieldwork locations along the Niagara Escarpment and highlighting the location of the white cedar (B2).

5. Discussion

This research attempts to examine the coupled relationship between plant communities and the evolving slope of the Niagara Escarpment in Hamilton by documenting vegetation characteristics and investigating a methodology for the documentation of tree sway. The main objective of this work is to determine how the growth of plants and movement of trees rooted in fractured bedrock affect slope stability, particularly along the upper portions of the escarpment. Documentation of the types of plant communities inhabiting different parts of the upper escarpment slope gives some insight into the degree of slope stabilization vegetation cover provides.

5.1 Vegetation Communities

Escarpment slope processes and their controls on vegetation have received less attention than other ecosystem processes such as fire, flooding, and windthrow when considering interactions at the landscape scale (Moss & Milne, 1998). Soil creep and debris slides have certainly contributed to the evolution of the Niagara Escarpment landscape and vegetation communities by facilitating the downslope movement of material which has modified underlying soil and bedrock profiles (Moss & Nickling, 1980; Moss & Milne, 1989). The downslope transition from mature forest plateaus to bedrock face and talus accumulation (Figure 13) occurs over short vertical distances resulting in abrupt changes in plant community structure. The two main study sites, along the Chedoke Radial Trail and the Rockcliffe Trail (Figure 1), also show considerable variability in the dominant species present on different parts of the slope profile, with coniferous species, such as white cedar (*Thuja occidentalis*), only being present on the upper plateau and bedrock face of the Rockcliffe Trail.

Previous research suggests that dense forest communities, such as those present on the upper plateaus of the escarpment in Hamilton, are intensely competitive for light, while understory plants have a more robust tolerance for shade (Larson *et al.*, 1989). Plant species competitiveness has also been correlated to a disturbance intolerance, implying that woodland forests may be particularly sensitive to physical disturbances imposed by both natural causes and human activity (Larson *et al.*, 1989). Hence, areas of disturbance on the upper forested plateau of the escarpment, such as along trails and roadways, should be carefully monitored due to the vulnerability of plant

species in these areas. At each of the research sites investigated in this study, there appeared to be little revegetation on exposed bedrock, especially where there was evidence of a recent rockfall, or surface water drainage over the slope. Some stress-tolerant species such as white cedar (*Thuja occidentalis*) can establish on weathered bedrock, but it is difficult to improve the stability of the bedrock face using vegetation growth and bioengineering processes (Moss & Milne, 1989). Improving the stability of the escarpment using vegetation should therefore focus on the plateaus, ledges, and areas of talus accumulation.

In areas of the talus experiencing high levels of rockfall, there is often sparse vegetation cover due to the unstable growing environment. Below the upper plateau at the Rockcliffe Trail study site, large bedrock blocks covered the talus, producing an unsuitable area for the growth of larger vegetation such as shrubs and trees (Moss & Milne, 1998). However, when larger, mature trees are established on such slopes they can act as a barrier to downslope sediment movement, trapping larger blocks and incorporating them into the talus matrix (Moss & Milne, 1989). In areas where bedrock blocks form the main surface feature, shrubs and saplings grow on top of the blocks. Vegetation cover on talus slopes thus appears to vary both spatially according to underlying bedrock material and size, as well as temporally, given the length of time from the last rockfall or landslide. The nature of vegetation communities growing on different parts of the escarpment and their influence on physical processes operating on the slope is therefore important to consider when evaluating slope stability. Maintaining slope stabilization is imperative for preserving the integrity of human infrastructure crossing the Niagara Escarpment, particularly along steep talus slopes.

5.2 Slope Stabilization

Previous research has discussed the composition of terrestrial cliff ecosystems along the Niagara Escarpment (Moss & Milne, 1989; Moss & Nickling, 1980; Larson *et al.*, 1989; Larson & Kelly, 1991; Gerrath *et al.*, 2000). However, there is a surprising lack of contemporary research examining the interaction between vegetation and slope stability along the escarpment in Hamilton (Moss & Milne, 1989) considering the increasing number of erosional events affecting human infrastructure (van Dongen, 2014; Mitchell, 2022). Research outside of the Hamilton area has focused on the feasibility of using plant roots to mechanically reinforce soil on hillslopes (Enns *et al.*, 2002; Bochet *et al.*, 2009; Stokes *et al.*, 2009; Stokes *et al.*, 2014). Vegetation can increase

protection of the soil surface and soil fertility by enhancing biological activity but can also result in destabilization of the soil. For example, strong wind events that result in stem breakage or uprooting of tall trees, compromise slope integrity (Stokes *et al.*, 2014; Quine & Gardiner, 2007). However, plant species with particular rooting patterns can be utilized for specific slope stabilization objectives and may be used to mitigate erosion along the escarpment (Enns *et al.*, 2002; Bochet *et al.*, 2009; Stokes *et al.*, 2009; Stokes *et al.*, 2014).

5.2.1 *Tree growth on sloping ground*

Root architecture is an important consideration in terms of the way in which forces on the above-ground biomass are transferred into the ground. The shape of the root system determines the way in which these forces are distributed (Norris *et al.*, 2008). Symmetrical root systems often enhance stability, but trees on sloped topography usually develop asymmetrical root systems. While the processes which impact this growth form are contentious, researchers agree that root mass is often aligned with prevailing wind direction (Norris *et al.*, 2008; Soethe *et al.*, 2006; Nicoll *et al.*, 2006). Mechanical load from prevailing winds has been found to have a greater effect on root architecture than slope angle (Norris *et al.*, 2008). It was not possible to determine if root architecture of the trees used in this research showed any significant correlation to wind direction; however, tree bole shape does appear to be influenced by the slope of the escarpment (Figures 21-23). J-shaped deformation of the trunk affected all trees in this study and appeared to coincide with the position of the escarpment edge (Figures 21-23). While seemingly not indicative of the influence of wind direction, these examples of trunk deformation are good indicators of both soil creep (Pawlik & Šamonil, 2018) and other hillslope disturbance processes and could be utilized to monitor hillslope instability along the escarpment in Hamilton.

5.2.2 *Species Suitability*

Previous research by Stokes *et al.* (2014) suggests that “pioneer species”, such as poplar (*Populus sp.*), willow (*Salix sp.*), or birch (*Fagus sp.*), are arboreal species that can be used for rapid stabilization of sloped topography. These species are usually the first to colonize disturbed sites and are preferred due to their ease of propagation and lateral rooting systems. Future efforts

to stabilize soil covered hillslopes along the escarpment in Hamilton, should consider the use of pioneer species which are beneficial for improving soil adherence in areas of talus accumulation. Along the Chedoke Radial Trail in Hamilton, talus slopes that appeared to recover from previous slope failure were covered by a variety of deciduous species such as maple (*Acer sp.*), shrubs such as sumac (*Rhus typhina*), and groundcover such as goldenrod (*Solidago canadensis*). Along the Rockcliffe Trail, similar deciduous forests and vegetal communities were present on recovered slopes with the addition of various coniferous species such as white cedar (*Thuja occidentalis*). Similarly, in research by Moss & Milne (1989), sites that had recovered to a closed canopy were primarily comprised of poplar and aspen (*Populus sp.*), birch (*Fagus sp.*), maple (*Acer sp.*), and cedar (*Thuja sp.*). Coniferous species such as lodgepole pine (*Pinus contorta*) and western red cedar (*Thuja plicata*) have also been suggested for use in stabilizing slopes of finely textured materials (Enns *et al.*, 2002). Slope stabilization protocols for the Niagara Escarpment should therefore consider using a mixture of tree species of different ages, using grasses, such as sedges (*Carex sp.*) and shrubs, such as sumac (*Rhus typhina*), to stabilize topsoil, and establish trees, such as oak (*Quercus sp.*), to improve soil fixation deeper in the soil profile. Revegetation should be concentrated where material is deposited and especially at the base of the slope. While diverse vegetal communities appear to have maintained slope stability along the Chedoke Radial and Rockcliffe trails, in other areas along the escarpment instability is a significant issue that requires further intervention. One such intervention could be the use of soft engineering structures to improve soil stabilization.

The use of soft engineering structures may promote slope stability along areas of the escarpment experiencing regular small slope failures. Brush layers or wattle fencing can be constructed with wood or live plant cuttings and placed where slope instability and failure are anticipated. These structures should be installed with adequate time for plant material to develop sufficient strength to provide stability (Stokes *et al.*, 2014; Figure 24). Soft-engineering methods may be used to mitigate erosional processes particularly on the escarpment talus, and intermediary plateaus in Hamilton to prevent the failure of debris from the slope onto public trails and access roads (Figure 24 and Figure 3).

While the physiological characteristics of some vegetation types and their root systems are suitable for slope stabilization, trees and tree boles are particularly prone to movement (tilt) in response to wind; this movement may be transmitted from the tree bole into root systems that

penetrate bedrock, resulting in increased forces along bedrock discontinuities such as fractures and bedding planes (Figure 6 and Figure 7). These forces may enhance the aperture of fractures and can loosen blocks from exposed bedrock faces thus increasing slope instability.

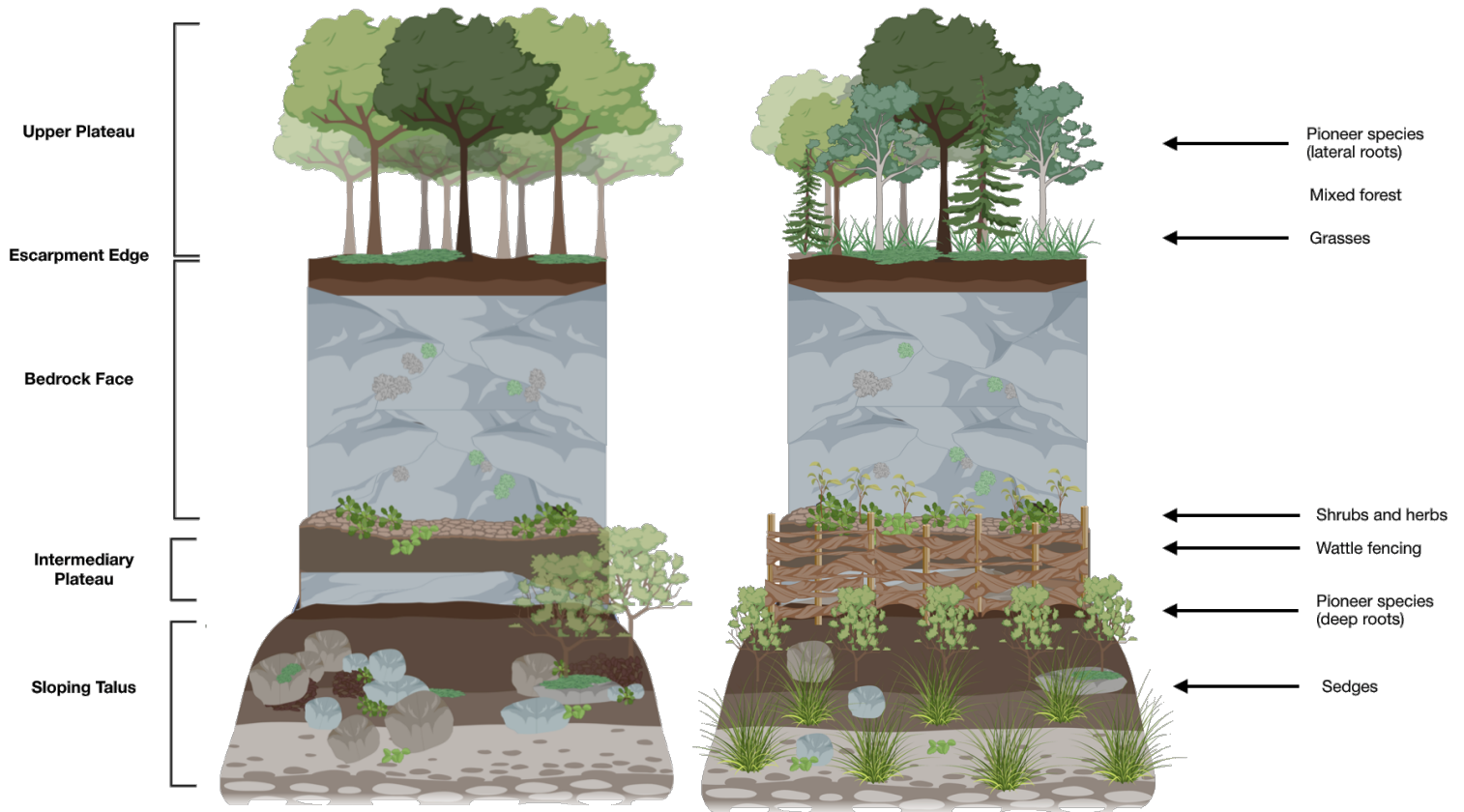


Figure 24: (Left) a simplified vertical transect of escarpment vegetation in Hamilton (not to scale). Patterns of plant growth and development can be related to the position on the escarpment: upper plateau, bedrock face, intermediary plateau (ledges), and sloping talus; (right) ideal distribution of vegetation species suitable for mitigating slope erosion along different positions of the escarpment (Created using BioRender.com).

5.3 Tree Bole Tilt

5.3.1 *Factors*

This research has documented accelerometer data suggesting that tree bole tilt is influenced by species type, wind direction, and wind speed, with strong contrasts in movement patterns between daytime and nighttime hours. The magnitude and pattern of tilt was determined to be significantly different for each of the three trees examined in this study (sugar maple, red oak, white cedar). While this relationship may be impacted primarily by species type, these results may also be affected by the geographic position of the studied trees along the escarpment as well as their position within the forest stand, and relationship to the dominant wind direction (Quine & Gardiner, 2007; Ciruzzi & Loheide II, 2019; Jimerson 2020). The dominant wind directions for the study dates were west-northwest and northwest, meaning that the wind passing through Hamilton was blowing toward the east-southeast or southeast (Figure 19). The weak correlation between cardinal wind direction and tree bole movement of the coniferous tree in this study was unexpected, given the highly exposed growth position of the white cedar along the escarpment (Table 4 and Figure 23). In contrast, there were strong correlations between tilt of the deciduous trees and wind direction (Table 4 and Figure 25). Air movement likely disturbed the canopies of the deciduous trees during leaf-gain, and branches during leaf-loss to a greater degree than that of the conifer, especially the sugar maple (R1) which faces into the wind (north). The conifer is growing on a south-facing slope, and tree bole movement was not significantly affected by winds from the northwest, despite an exposed growth position on the edge of the escarpment. Due to the strong correlation recorded here between deciduous tree bole tilt and dominant wind direction, trees growing on the escarpment that face into the wind may be particularly susceptible to the transmission of wind-induced movement from the bole into the root system (Jimerson, 2020); increased root forces could contribute to fracture enlargement and bedrock disaggregation. As wind direction in Hamilton fluctuates throughout the year, forest communities located along different areas of the escarpment would exert increased forces on underlying bedrock at different times, depending on their relationship to the dominant wind direction.

On most days of this study, an increase of tilt (movement) along the y- and z-axes recorded by the accelerometers tended to occur during daytime hours and coincided with periods of increased

wind speed, usually around midday (Figure 25). Research synthesized by Jackson *et al.* (2021) also found that maximum tree deflection (movement) increased with wind speed, while a study by Ciruzzi & Loheide II (2019) found that tree water content drove diurnal patterns of sway; there was a notable increase in sway period, or the amount of time needed for the crown of a tree to return to vertical after being deflected by wind, during the day. This increased sway period was associated with water stress and conversely, a decrease in sway period was associated with water recovery during the night. The daytime periods of increased wind speed identified in this study may amplify tree sway and forces transmitted from the tree bole into root systems in underlying escarpment bedrock, potentially contributing to fracture expansion and enhanced bedrock disaggregation.

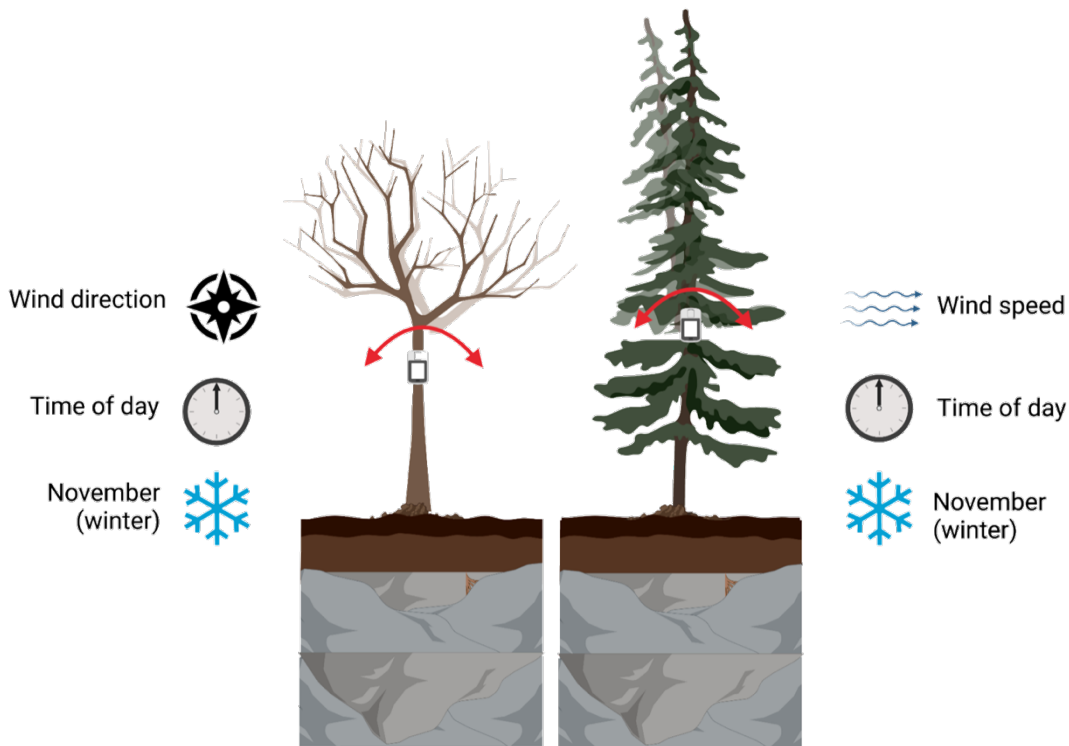


Figure 25: Main factors impacting the tree bole tilt for deciduous species (left) and coniferous species (right) investigated in this study. Wind direction was most strongly correlated to tree bole tilt of deciduous trees, whereas wind speed was most strongly correlated to tilt along the bole of the coniferous tree. Tilt was generally greatest around mid-day, and had the strongest impact on all monitored trees during the study dates in November (Created using BioRender.com).

All trees in this study experienced a strong correlation between tilt and high wind speeds during the study dates in November (Table 3 and Figure 16). Freezing temperatures, common during months such as November, have been noted to increase the frequency of tree sway (Granucci *et al.*, 2012). The elastic properties of tree wood have been shown to decrease under freezing conditions, causing trees to oscillate at a higher frequency (Granucci *et al.*, 2012). Therefore, during the months that experience temperatures below freezing, trees along the escarpment in Hamilton may be at greater risk of upturning or stem breakage due to a higher frequency of tree sway (Figure 25).

In contrast, tilt of the deciduous sugar maple tree bole appeared most closely connected to wind speed during the study dates in May (Figure 18). This finding is supported by research synthesized by Jackson *et al.* (2021), who found that greatest tree sway occurred in the summer season primarily for deciduous trees. This may be due to the fullness of deciduous tree canopies particularly during the summer. Tree canopy cover (CaCo) documented in this research varied significantly throughout the study period, with maximum coverage in May, and minimum in March (Figure 20). Previous studies speculate that increased deflection of deciduous trees in the summer season is likely in response to their increased leaf mass, creating a larger sail area and resulting in increased drag forces (Jackson *et al.*, 2021; Dellwik *et al.*, 2019; Theckes *et al.*, 2011; Moore *et al.*, 2018). Deciduous trees may therefore experience a higher degree of canopy deflection compared to coniferous trees in the summer season, resulting in increased bole movement and the potential movement of rooting systems. This finding is also supported by Jimerson (2020) who documented that tree species exerted higher forces into underlying bedrock during warmer seasons and during periods of rainfall occurring over consecutive days. Although rainfall amounts and humidity were not documented in this study, it is postulated here that warm and wet conditions will compound the effects of both chemical and mechanical weathering processes on the escarpment bedrock, increasing the potential for slope failure (Eppes & Keanini, 2017; Jimerson, 2020).

5.4 Conclusions

5.4.1 *Major Findings*

This research aims to explore methods for quantifying the impacts of plant growth on highly fractured bedrock along the Niagara Escarpment in the Hamilton region. The specific objectives are to document how the escarpment slope impacts vegetation growth, to monitor tree bole movement in response to wind and its potential impact on underlying bedrock, and to consider how species characteristics affected the magnitude of wind-driven movements of trees. Results of this research add to the current understanding of plant ecosystem dynamics impacting the Niagara Escarpment and can provide better insight into erosional processes that operate on this important geomorphic feature (Figure 26).

Vegetation growth appears to be closely related to position on the vertical slope of the escarpment and has resulted in the formation of distinct vegetal communities. Escarpment vegetation transitions downslope from mature forest on the upper plateau to exposed bedrock on the steepest faces, and shrub-dominated communities on areas of talus accumulation (Figure 13). Mature forest areas on the upper and intermediary plateaus may be most at risk of instability and acute failure as a result of both natural and human causes, due to the overlying, highly fractured escarpment caprock (Figure 4), as well as current and future human infrastructure and foot traffic along unstable ecological areas. Slope instability on areas of talus accumulation may be mitigated by encouraging the growth of species such as sedges (*Carex sp.*) and sumac (*Rhus typhina*), which are known to enhance topsoil stabilization.

Daily patterns of tree tilt monitored by the accelerometers appeared to be primarily controlled by the diurnal variability of wind, as tree bole movement was strongly correlated with high wind speeds during daylight hours. However, despite obtaining data to show tree bole movement is affected by wind patterns, it still remains unclear how tree bole movement is transferred to root systems and can impact processes of bedrock disaggregation along the escarpment. This clearly requires further investigation (Figure 26).

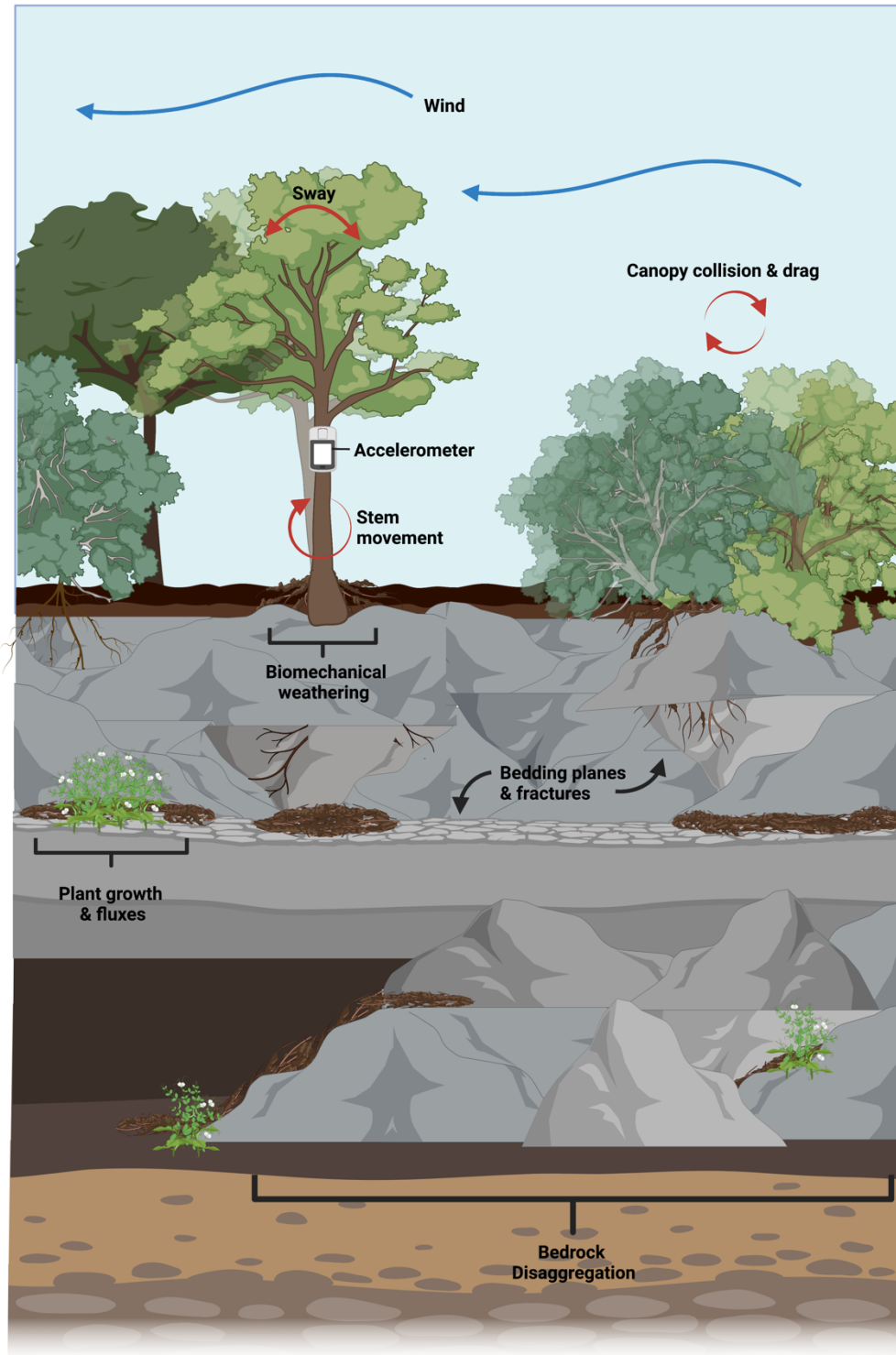


Figure 26: Schematic diagram showing potential environmental factors impacting erosional processes on the Niagara Escarpment in Hamilton, with a particular focus on vegetation growth in bedrock discontinuities and associated weathering processes, and tree sway movement during periods of wind excitation documented using triaxial accelerometers (Created using BioRender.com).

The data collected in this study indicate that tree bole tilt was significantly different for each tree species monitored. Tilt was most significantly correlated to wind speed for the white cedar coniferous tree, while tilt was most significantly correlated to wind direction for the sugar maple and red oak deciduous trees. The movement of trees growing on slopes facing into the dominant wind direction, such as the sugar maple and red oak in this study, will be strongly impacted by wind characteristics, and may experience greater movement compared to trees growing in more sheltered areas facing away from the wind. In the month of November, both coniferous and deciduous tree species monitored in this study showed a strong relationship between tree bole tilt and wind speed; this suggests that trees growing along the edge of the escarpment may be most susceptible to wind-induced movement and potential failure in the winter months (November to March).

Canopy coverage also appears to have had some influence on the amount of tree bole movement documented in this study. Canopy coverage was greatest during the month of May, and least during the month of March for all trees examined in this study. In May, tilt of the deciduous sugar maple tree bole appeared to exhibit a particularly strong correlation to wind speed; this may reflect the greater canopy coverage and larger sail area of the maple tree in comparison to the red oak and coniferous white cedar at this time.

The results of this investigative study add to the findings of previous literature examining the impacts of vegetation on geomorphological processes along the Niagara Escarpment (Figure 26). These findings suggest that certain vegetal communities along the escarpment may help reduce slope failure events, and by encouraging the growth of certain plant species, slope instability may be mitigated in certain areas. This research also suggests that the dissipation of wind energy varies significantly for different tree species in different areas of the escarpment in Hamilton, but that all trees may be particularly vulnerable to high amounts of movement in the winter months and could potentially enhance bedrock erosion. However, certain limitations to this research may impact the application of these results to different areas of the escarpment in Hamilton and elsewhere.

5.4.2 *Limitations*

This research was conducted under conditions allowing limited access to field sites during the COVID-19 pandemic of 2020-2021. Hence the cataloguing of plant species, particularly trees and shrubs, at the two selected study sites, Chedoke Radial Trail, and Rockcliffe Trail, was conducted under conditions of restricted field access and should not be considered as a full inventory of the vegetation present on the upper parts of the escarpment. However, the catalogue presented here is considered to be sufficient for the purposes of this study.

The research presented in this thesis also represents a pilot study for the use of triaxial accelerometers to quantify the impacts of tree tilt on forces contributing to root movement that could enhance bedrock erosion through fracture expansion. The inherent complexity of using an untested approach to answer a multifaceted question related to erosion of the escarpment, presented many limitations to this study (Appendix B). Firstly, the use of low-cost AL101 sensors is not ideal for the accurate measurement of tree bole movement over extended periods as they are not designed to provide long-term records with precision. However, they do offer many benefits, such as being relatively simple to install with little disturbance of the tree being monitored, and they do allow measurements to be collected in a simple manner. While the accelerometer measurements obtained from the tree boles are not particularly precise, and do not allow the magnitude of forces transmitted to root systems and underlying bedrock to be accurately determined, they do provide an estimate of the magnitude of tilt experienced along the tree bole under variable conditions. This does provide some estimate of the amount of forcing that may be translated into belowground biomass. Unfortunately, these limitations do restrict the application of results from this study as it remains unclear how much tree bole movement translates down into root systems and impacts fracture growth and bedrock erosion. Future research should focus on documenting the translation of wind-induced movement from the tree bole into the rooting systems of various forms of vegetation cover on the escarpment.

5.4.3 Future Research

The initial findings of the research reported here have allowed the identification of several areas of future research that will better quantify the impact of tree growth on fractured escarpment bedrock.

1) A more holistic view of forces exerted by tree roots on underlying bedrock can be obtained by augmenting accelerometer data with data collected from piezometric force sensors which can be used to record the force of tree root growth and expansion at the root-rock interface (e.g., Jimerson, 2020). Incorporating force sensors into a field study will provide additional information regarding the forces acting on bedrock discontinuities from the below-ground biomass. This will contribute to the understanding of how forces created by tree growth and movement are translated to fractured bedrock and their potential impact on slope stability.

2) A future study should determine if position within the forest stand is a significant factor impacting mechanisms of tree sway along the escarpment in Hamilton. This study has only examined trees within an established forest canopy and has not examined the effects of wind-induced fluctuations on standalone trees. Previous research synthesized by Jackson *et al.* (2021) determined that tree position significantly impacted tree sway frequency. This direction of research may identify areas of forest along the escarpment most at risk of increased swaying and the potential for inducing slope failure.

3) It would be beneficial to obtain information about hydrological conditions, including soil moisture, that affect tree growth along the escarpment. Previous research by Ciruzzi & Loheide II (2019) highlights the importance of water availability on the movement of trees and suggests a strong correlation between water-stress and increased tree sway frequency. Periods of increased water uptake also result in the enlargement of tree roots and increased forces on underlying bedrock (Jimerson *et al.*, 2020). Therefore, soil moisture and water-uptake may be important for determining frequency of bedrock disaggregation along the escarpment.

This thesis presents an initial exploration of the dynamic relationships between vegetation growth and active geomorphic processes on the Niagara Escarpment in Hamilton, Ontario. The Niagara Escarpment is a dynamic feature, subject to continual erosion, and any slope remediation and protection plans should carefully consider the use of selected vegetation plantings and the installation of soft engineering systems to protect vulnerable slopes.

BIBLIOGRAPHY

- Anderson, R. S., Rajaram, H., & Anderson, S. P. (2019). Climate driven coevolution of weathering profiles and hillslope topography generates dramatic differences in critical zone architecture. *Hydrol. Process.*, 33: 4–19.
- Armstrong, D.K., Dodge, J.E.P. (2007). Paleozoic Geology of Southern Ontario; Ontario Geological Survey, Miscellaneous Release – Data 219.
- Barlow, J. (2002). Creep and the development of Niagara cuesta. *Earth Surf. Proc. Land.*, 27: 1125-1135.
- Bernard, J.M. (1990). Life history and vegetative reproduction in *Carex*. *Can. J. Bot.* 68: 1441-1448.
- Bochet E., García-Fayos, P., Poesen, J. (2009). Topographic thresholds for plant colonization on semi-arid eroded slopes. *Earth Surf. Proc. Land.*, 34: 1758-1771.
- Bourguet, R., Triantafyllou, M. S. (2016). The onset of vortex-induced vibrations of a flexible cylinder at large inclination angle. *J. Fluid Mech.*, 809:111-134.
- Brantley, S. L., Megonigal, J. P., Scatena, F. N., Balogh-Brunstad, Z., Barnes, R. T., Bruns, M. A., Van Cappellen, P., Dontsova, K., Hartnett, H. E., Hartshorn, A. S., Heimsath, A., Herndon, E., Jin, L., Keller, C. K., Leake, J. R., Mcdowell, W. H., Meinzer, F. C., Mozdzer, T. J., Petsch, S., Pett-Ridge, J., Pregitzer, K. S., Raymond, P. A., Riebe, C. S., Shumaker, K., Sutton-Grier, A., Walter, R., Yoo, K. (2011). Twelve testable hypotheses on the geobiology of weathering. *Geobiology*, 9: 140-165.
- Brett, C.E., Goodman, W.M., Loduca, S.T., Tetreault, D. (1999). Silurian-early Devonian sequence stratigraphy, events, and paleoenvironments of western New York and Ontario, Canada.
- Brunton, F.R., Brintnell, C. (2020). Early Silurian sequence stratigraphy and geological controls on karstic bedrock groundwater-flow zones, Niagara Escarpment region and the subsurface of southwestern Ontario; report [PDF document] in Ontario Geological Survey, Groundwater Resources Study 13.
- Chellali F., Khellaf, A., Belouchrani, A. (2013). Identification and analysis of wind speed patterns extracted from multi-sensors measurements. *Stoch. Environ. Res. Risk Assess.*, 27:1-9.
- Ciruzzi, D.M., Loheide II, S.P. (2019). Monitoring tree sway as an indicator of water stress. *Geophys. Res. Lett.*, 46: 12,021–12,029.
- Cox, J.E. & Larson, D.W., 1992. Spatial heterogeneity of vegetation and environmental factors on talus slopes of the Niagara Escarpment. *Can. J. Bot.*, 71: 323-332.

- Crins, W.J. (2009). The ecosystems of Ontario – Part 1: ecozones and ecoregions. Environment & Energy, Ontario.ca. Retrieved from: <https://www.ontario.ca/page/ecosystems-ontario-part-1-ecozones-and-ecoregions>
- Dellwik, E., van der Laan, M.P., Angelou, N., Mann, J., Sogachev, A. (2019). Observed and modeled near-wake flow behind a solitary tree. *Agr. Forest Meteorol.*, 265: 78-87.
- Dickinson, R., Royer, F. (2021). Plants of Southern Ontario: Trees, Shrubs, Wildflowers, Grasses, Ferns & Aquatic Plants. Lone Pine Media Productions Ltd., British Columbia, 527p.
- Enns, K.A., Huff, V., Canning, C., Lucas, E. (2002). A property owner's guide to controlling erosion using native vegetation for Arrow Lakes. PDF File prepared for B.C. Hydro. B.C. Larkspur Biological Consultants Ltd., Castlegar, B.C. 86p.
- Eppes, M.C, Keanini, R. (2017). Mechanical weathering and rock erosion by climate-dependent subcritical cracking. *Rev. Geophys.*, 55: 470-508.
- Gardiner, B. A. (1992). Mathematical Modelling of the Static and Dynamic Characteristics of Plantation Trees, in J. Franke and A. Roeder (eds.), *Mathematical Modelling of Forest Ecosystems*, Sauerlanders, Verlag, Frankfurt am Main, pp. 40-61.
- Ghestem, M., Sidle, R.C., Stokes, A. (2011). The Influence of Plant Root Systems on Subsurface Flow: Implications for Slope Stability. *BioScience*, 61: 869-879.
- Gerrath, J.F., Gerrath, J.A., Matthes, U., Larson, D.W. (2000). Endolithic algae and cyanobacteria from cliffs of the Niagara Escarpment, Ontario, Canada. *Can. J. Bot.*, 78: 807-815.
- Granucci, D., Rudnicki, M., Hiscox, A., Miller, D., Hong-Bing, S. (2013). The effects of freezing on tree sway frequencies. *Agr. Forest Meteorol.*, 168: 10-14.
- Hamilton Conservation Authority (HCA). (2011). Planning & Regulation Policies and Guidelines; HCA. Retrieved from: <https://conservationhamilton.ca/images/PDFs/Planning/PlanRegPolicyGuidewAppendices.pdf>
- Hassinen, A., Lemettinen, M., Peltola, H., Kellomaki, D., Gardiner, B.A. (1998). A prism-based system for monitoring the swaying of trees under wind loading. *Agric. Forest Meteorol.*, 90: 187–194.
- Hayakawa, Y.S., Matsukura, Y. (2010). Stability analysis of waterfall cliff face at Niagara Falls: An implication to erosion mechanisms of waterfall. *Eng. Geol.*, 116: 178-183.
- Hayati, E., Abdi, E., Saravi, M.M., Nieber, J.L., Majnounian, B., Chirico, G.B., Wilson, B., & Nazarirad, M. (2018). Soil water dynamics under different forest vegetation cover: Implications for hillslope stability. *Earth Surf. Proc. Land.*, 43: 2106-2120.

- Hewitt, D.F. (1971). The Niagara Escarpment; Ontario Geologic Survey, Industrial Mineral Report No. 35, 71p.
- Jackson, T.D., Sethi, S., Dellwik, E., Angelou, N., Bunce, A., van Emmerik, T., Duperat, M., Ruel, J.C., Wellpott, A., Van Bloem, S., Achim, A., Kane, B., Ciruzzi, D.M., Loheide II, S.P., James, K., Burcham, D., Moore, J., Schindler, D., Kolbe, S., Wiegmann, K., Rudnicki, M., Lieffers, V.J., Selker, J., ... Gardiner, B. (2021). The motion of trees in the wind: a data synthesis. *Biogeosciences*, 18:4059-4072.
- James, K., Hallam, C., Spences, C. (2013). Measuring tilt of tree structural root zone under static and wind loading. *Agr. Forest Meteorol.*, 168: 160-167.
- Jiang, Z., Liu, H., Wang, H., Peng, J., Meersmans, J., Green, S.M., Quine, T.A., Wu, X., Song, Z. (2020). Bedrock geochemistry influences vegetation growth by regulating the regolith water holding capacity. *Nat. Commun.*, 11:2392.
- Jimerson, C. R. (2020). Environmental Influences on Tree-driven Karst Bedrock Physical Weathering. Graduate Theses and Dissertations Retrieved from <https://scholarworks.uark.edu/etd/3807>
- Larson, D.W., Kelly, P.E. (1991). The extent of old growth *Thuja occidentalis* on cliffs of the Niagara Escarpment. *Can. J. Bot.*, 69: 1628-1636.
- Larson, D.W., Spring, S.H., Matthes-Sears, U., Bartlett, R.M. (1989) Organization of the Niagara Escarpment cliff community. *Can. J. Bot.*, 67: 2731-2742.
- Lee, R. (2022). Delineation and analysis of active geomorphological processes using high resolution spatial surveys. *MacSphere, Open Access Dissertations and Theses*. Retrieved from: <http://hdl.handle.net/11375/27445> .
- Malik, I., Pawlik, Ł, Ślęzak, A., Wistuba, M. (2019) A study of the wood anatomy of *Picea abies* roots and their role in biomechanical weathering of rock cracks. *Catena*, 173: 264-275.
- Mitchell, D. (2022). ‘Erosion concerns’ set to close Sydenham escarpment access in Hamilton. Global News, Retrieved from: <https://globalnews.ca/news/8619391/close-sydenham-escarpment-hamilton/>.
- Marshall, J.A. (2018). From ice to trees, surprising insights into past and present processes that sculpt our earth: AGU Fall Meeting Abstracts, v. 44, <http://adsabs.harvard.edu/abs/2018AGUFMEP44A..01M>.
- Matthes-Sears, U., Larson, D.W. (1995). Rooting Characteristics of Trees in Rock: A Study of *Thuja occidentalis* on Cliff Faces. *Int. J. Plant Spec.*, 156: 679-686.
- Moore, J., Gardiner, B., Sellier, D., (2018). Tree mechanics and wind loading, in: *Plant Biomechanics*, Springer International Publishing, Cham, p.79-106.
- Moses, C., Robinson, D., Barlow, J. (2014). Methods for measuring rock surface weathering and erosion: A critical review. *Earth-Sci. Rev.*, 135: 141-161.

- Moss, M.R., Milne, R.J. (1998). Biophysical processes and bioregional planning: The Niagara Escarpment of southern Ontario, Canada. *Landscape Urban Plan.*, 40: 251-268.
- Moss, M.R. & Nickling, G., 1980. Geomorphological and vegetation interaction and its relationship to slope stability on the Niagara Escarpment, Bruce Peninsula, Ontario. *Géogr. Phys. Quatern.*, 24: 95-106.
- Nicoll B.C., Berthier S., Achim A., Gouskou K., Danjon F., van Beek L.P.H. (2006). The architecture of *Picea sitchensis* structural root systems on horizontal and sloping terrain. *Trees-Struct. Funct.*, 20: 701-712.
- Nie, Y., Chen, H., Ding, Y., Yang, J., & Wang, K. (2017). Comparison of Rooting Strategies to Explore Rock Fractures for Shallow Soil-Adapted Tree Species with Contrasting Aboveground Growth Rates: A Greenhouse Microcosm Experiment. *Front. Plant Sci.*, 8:1651.
- Norris, J.E., Stokes, A., Mickovski, S.B., Cammeraat, E., van Beek, R., Nicoll, B.C., & Achim, A. (2008). Slope Stability and Erosion Control: Ecotechnological Solutions. Springer, Dordrecht, Netherlands, 288p.
- Parker, K. C., & Bendix, J. (1996). Landscape-scale geomorphic influences on vegetation patterns in four environments. *Phys. Geogr.*, 17: 113-141.
- Pawlik, Ł, Phillips, J.D., Šamonil, P. (2016) Roots, rock, and regolith: Biomechanical and biochemical weathering by trees and its impact on hillslopes—A critical literature review. *Earth-Sci. Rev.*, 159: 142-159.
- Peltola, H. (1996). Swaying of trees in response to wind and thinning in a stand of Scots pine. *Boundary-Layer Meteorology*, 77: 285-304.
- Pérez, F. (2012). Biogeomorphological influence of slope processes and sedimentology on vascular talus vegetation in the southern Cascades, California. *Geomorphology*, 138: 29-48.
- Phillips, J.D., Turkington, A.V., Marion, D.A. (2008). Weathering and vegetation effects in early stages of soil formation. *Catena*, 72: 21-28.
- Quine, C.P., Gardiner, B.A. (2007). 'How the Interaction of Wind and Trees Results in Wind-throw, Stem Breakage, and Canopy Gap Formation', in Johnson, E.A., Miyanishi, K. (Eds.) (2007). *Plant disturbance ecology: The process and the response*. Retrieved from <https://ebookcentral.proquest.com>
- Richter, D.D, Billings, S.A. (2015). One physical system: Tansley's ecosystem as Earth's critical zone. *New Phytol.*, Retrieved from <https://doi.org/10.1111/nph.13338>.

- Rodie, A., Post, R. (2009). Niagara Escarpment Baseflow Study; Niagara Escarpment Commission. Retrieved from: <https://www.nvca.on.ca/Shared%20Documents/Niagara%20Escarpment%20Baseflow%20Study%202009.pdf>.
- Rudnicki, M., Silins, U., Leiffers, V.J., Josi, G. (2001). Measure of simultaneous tree sways and estimation of crown interactions among a group of trees. *Trees*, 15: 83-90.
- Schwinning, S. (2020). A critical question for the critical zone: how do plants use rock water? *Plant Soil*, 454: 49-56.
- Sellier, D., Soulier, D., Fourcaud, T., Brunet, Y. (2003). The Venfor Project: influence of the aerial architecture on tree swaying – an experimental approach. In: Ruck, B. (Ed.), *Wind effects in trees*, University of Karlsruhe, Germany.
- Soethe N., Lehmann J., Engels, C. (2006). Root morphology and anchorage of six native tree species from a tropical montane forest and an elfin forest in Ecuador. *Plant Soil*, 279: 173–185.
- Stokes, A., Atger, C., Bengough, A.G., Fourcaud, T., Sidle, R.C. (2009). Desirable plant root traits for protecting natural and engineered slopes against landslides. *Plant Soil*, 324: 1–30.
- Stokes, A., Douglas, G. B., Fourcaud, T., Giadrossich, F., Gillies, C., Hubble, T., Kim, J. H., Loades, K. W., Mao, Z., McIvor, I. R., Mickovski, S. B., Mitchell, S., Osman, N., Phillips, C., Poesen, J., Polster, D., Preti, F., Raymond, P., Rey, F., ... Walker, L. R. (2014). Ecological mitigation of Hillslope instability: Ten key issues facing researchers and practitioners. *Plant Soil*, 377: 1–23.
- Straw, A. (1968). Late Pleistocene glacial erosion along the Niagara Escarpment of southern Ontario. *Bull. Geol. Soc. Am.*, 79: 889-910.
- Theckes, B., de Langre, E., Boutillon, X. (2011). Damping by branching: a bioinspiration from trees. *Bioinspir. Biomim.*, 6.
- Tovell, W.M. (1992). Guide to the geology of the Niagara Escarpment, with field trips; Niagara Escarpment Commission (and Ontario Heritage Foundation), Ashton-Potter Ltd., Concord, Ontario, 159p., including Field trips A-J, appendixes, and index.
- Van Dongen, M. (2016). Claremont Access lanes closed indefinitely after ‘slope movement’. [HamiltonNews.com](https://www.hamiltonnews.com/news-story/6995666-claremont-access-lanes-closed-indefinitely-after-slope-movement/), retrieved from: <https://www.hamiltonnews.com/news-story/6995666-claremont-access-lanes-closed-indefinitely-after-slope-movement/>.
- Van Emmerik, T., Steele-Dunne, S., Hut, R., Gentine, P., Guerin, M., Oliveira, R.S., Wagner, J., Selker, J., van de Giesen, N. (2017). Measuring Tree Properties and Responses Using Low-Cost Accelerometers. *Sensor*, 17: 1098.

Wang, Z., Wang, G., Li, C., Wang, F. (2005). A preliminary study on vegetation-erosion dynamics and its applications. *Sci. China Ser. D*, 48, 689-700.

Wang, A., Yang, X., Xin, D. (2022). The Tracking and Frequency Measurement of the Sway of Leafless Deciduous Trees by Adaptive Tracking Window Based on MOSSE. *Forests*,13: 81.

APPENDICES

APPENDIX A. Accelerometer Discrepancies

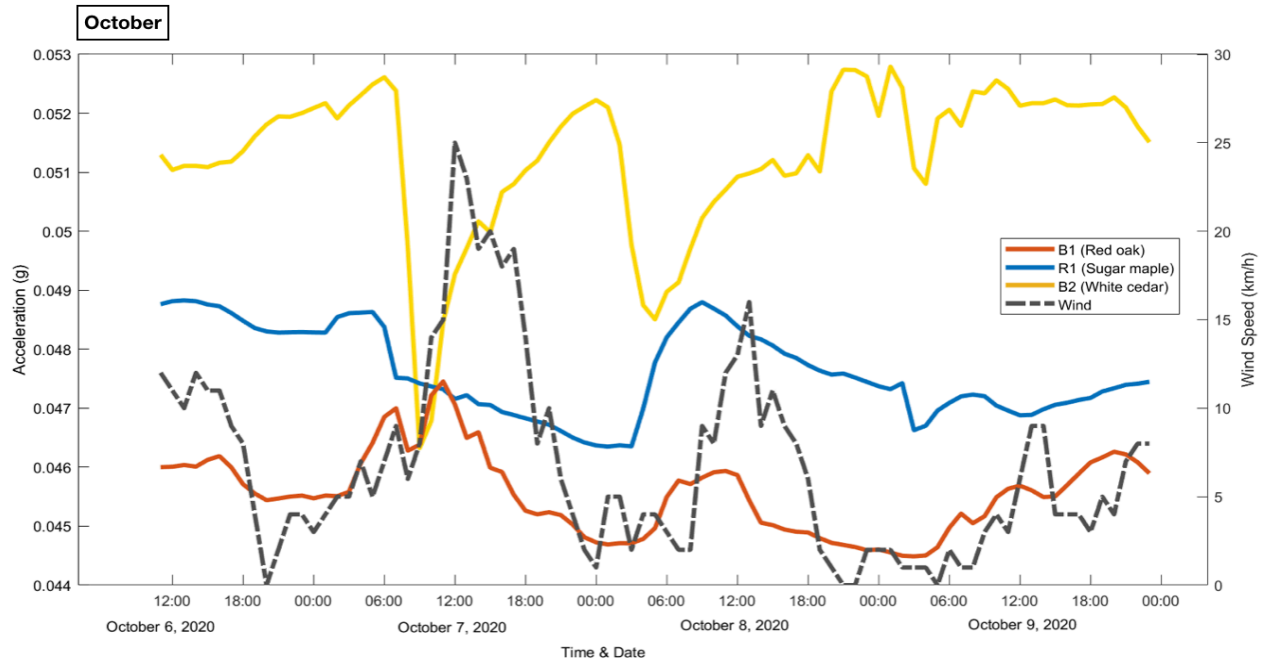


Figure A-1: The relationship between acceleration along the y- and z-axes and wind speed for the studied days in the month of October. Tree bole tilt is depicted by acceleration(g) for unit B1(red), unit B2 (yellow), and unit R1(blue). Wind speed (km/h) is indicated by the dashed grey line. Increased tilt along the y- and z-axes are indicated by increasing values of acceleration(g).

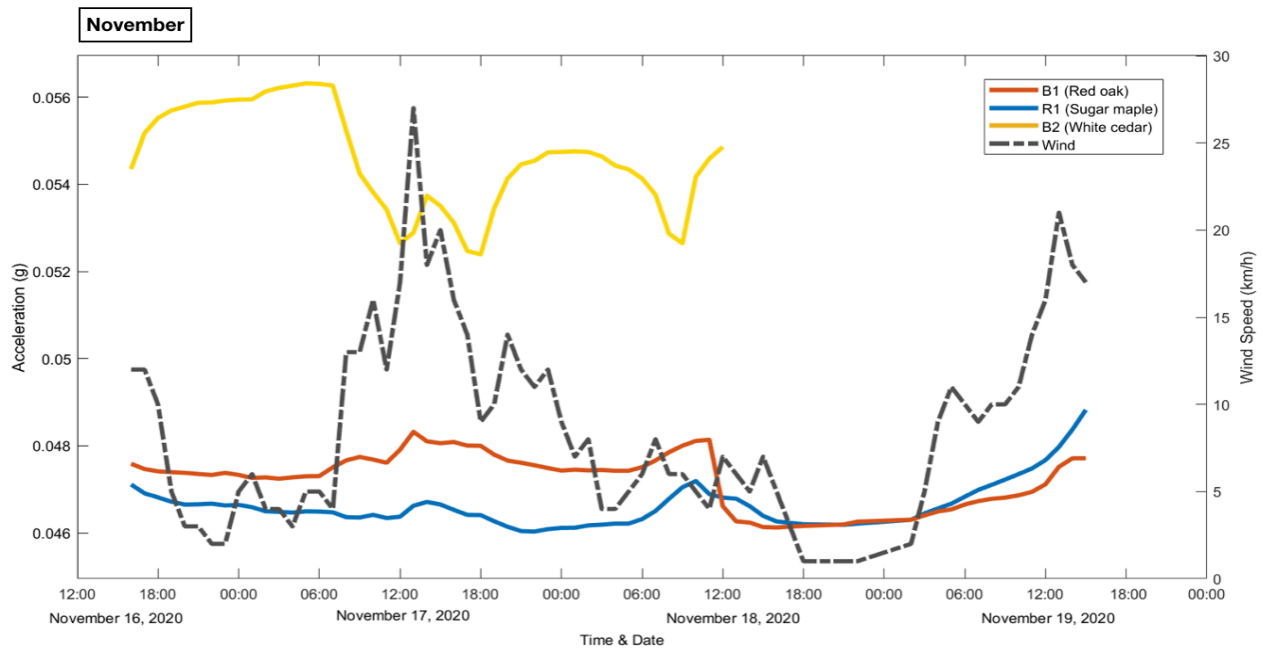


Figure A-2: The relationship between acceleration along the y- and z-axes and wind speed for the studied days in the month of November. Tree bole tilt is depicted by acceleration(g) for unit B1(red), unit B2 (yellow), and unit R1(blue). Wind speed (km/h) is indicated by the dashed grey line. Increased tilt along the y- and z-axes are indicated by increasing values of acceleration(g). Unit B2 (yellow) covers a shorter period of time due to an issue of battery-life.

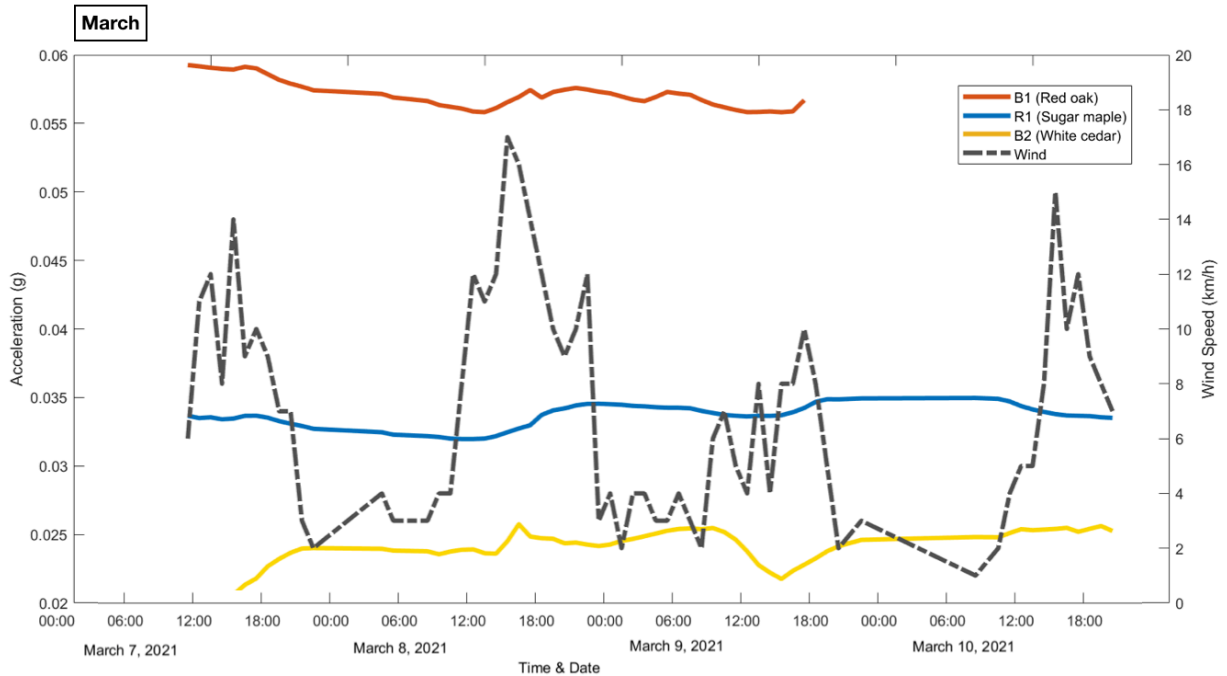


Figure A-3: The relationship between acceleration along the y- and z-axes and wind speed for the studied days in the month of March. Tree bole tilt is depicted by acceleration(g) for unit B1(red), unit B2 (yellow), and unit R1(blue). Wind speed (km/h) is indicated by the dashed grey line. Increased tilt along the y- and z-axes are indicated by increasing values of acceleration(g). Unit B1 (red) covers a shorter period of time due to an issue of battery-life.

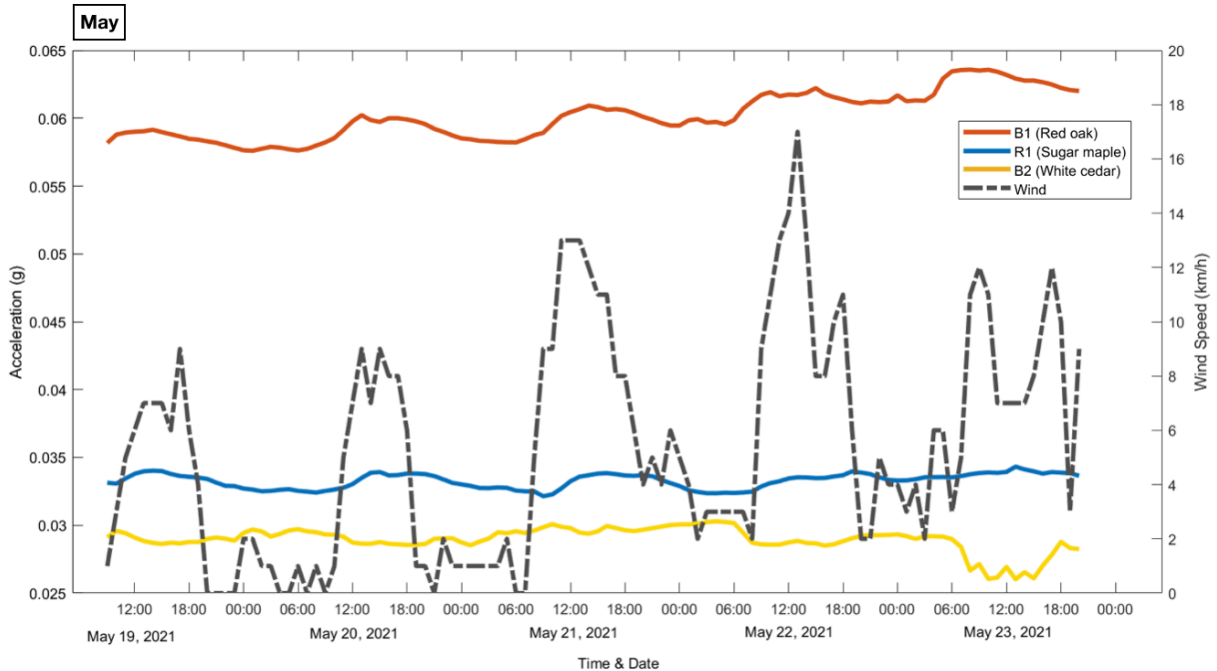


Figure A-4: The relationship between acceleration along the y- and z-axes and wind speed for the studied days in the month of May. Tree bole tilt is depicted by acceleration(g) for unit B1(red), unit B2 (yellow), and unit R1(blue). Wind speed (km/h) is indicated by the dashed grey line. Increased tilt along the y- and z-axes are indicated by increasing values of acceleration(g).

APPENDIX B. Accelerometer Limitations

1. Weather data used in this study were obtained from an already established weather station in Hamilton which was not in close proximity to either of the study sites (Figure 1). The geographic distance of the weather station from the study sites leaves room for error due to the possibility of different wind directions and speeds directly affecting the study sites.
2. The AL101s recorded tilt values at one second intervals, whereas wind speed and direction were recorded hourly at the weather station. This leaves room for greater number of errors when correlating averaged hourly tilt records with wind characteristics and may have resulted in a reduction of the number of resonance or sway periods recorded.
3. There were several issues encountered during the accelerometer installation processes that compromised the recorded data. Trees are continually moving in the wind which made it difficult to determine the initial trunk position in a windless state. This research limitation was also acknowledged by Wang *et al.* (2022). Therefore, results presented in this research simply identify the magnitude of change rather than absolute displacement over time. As well, it is difficult to discern if measured tilt recorded by the AL101s is indicative of tilt for the whole tree, or if these are only indicative of tilt along part of the tree. It is likely that different areas of the trees in this research behaved differently during wind events, and future studies should consider synchronous measurements along several segments of a tree.
4. Additional physical phenomena that may have affected the recorded tree bole movements, such as the wind flow-induced vibrations leading to amplified drag forces on trees (Strouhal vortex shedding; Bourguet & Triantafyllou, 2016), were not considered when analyzing data obtained from the AL101 units. Therefore, a number of factors related to wind dynamics that may also play a role in affecting tilt of the tree bole, should be considered in any future research.